NASA TECHNICAL NOTE

ANALYSIS OF CHARRING ABLATION WITH DESCRIPTION OF ASSOCIATED COMPUTING PROGRAM

by Fred W. Matting

Ames Research Center
Moffett Field, Calif. 94035

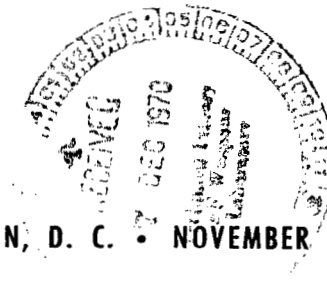

NATIONAL AERONAUTICS AND SPACE ADMINISTRATION • WASHINGTON, D. C. • NOVEMBER 1970

1. Report No. NASA TN D-6085	2. Government Accession No.	3. Recipie
4. Title and Subtitle ANALYSIS OF CHARRING ABLATION WITH DESCRIPTION OF ASSOCIATED COMPUTING PROGRAM		5. Report Date November 1970 6. Performing Organization Code
7. Author(s) Fred W. Matting		8. Performing Organization Report No. A-3614
9. Performing Organization Name and Address NASA Ames Research Center Moffett Field, Calif., 94035		10. Work Unit No. 124-07-01-10-00-21 11. Contract or Grant No.
12. Sponsoring Agency Name and Address National Aeronautics and Space Administration Washington, D. C., 20546		13. Type of Report and Period Covered Technical Note 14. Sponsoring Agency Code
15. Supplementary Notes		

16. Abstract

A general method is presented for solving the problem of heat-shield response in the stagnation region of a charring type ablator. The analysis is actually for the stagnation point of an axisymmetric blunt body, but it is a valid approximate method for calculations in the stagnation region of any arbitrary blunt body. The analysis is applicable to wind-tunnel or flight conditions, and the heat loadings are either arbitrarily assigned or they are calculated concurrently with the heat-shield response. Surface heating (or cooling) mechanisms accounted for are those due to convection, radiation, homogeneous combustion, heterogeneous combustion, surface material removal by means other than combustion (includes erosion), and sublimation. Physical and thermodynamic properties of the ablating material are arbitrarily assigned so that calculations can be made for various materials.

A typical application of the analysis is given as an illustration. The analysis is machine programmed for numerical solutions using a finite difference scheme, and a family of computing programs is used. These programs are described and instructions are provided for using them. The programs can be obtained from COSMIC, University of Georgia, Athens, Georgia, 30601.

17. Key Words (Suggested by Author(s)) Ablation Heat shields, response Heat shield materials (charring) Pyrolysis and charring Thermal protection	18. Distribution Statement Unclassified-Unlimited

19. Security Classif. (of this report) Unclassified	20. Security Classif. (of this page) Unclassified	21. No. of Pages 84	22. Price* $3.00

*For sale by the Clearinghouse for Federal Scientific and Technical Information
Springfield, Virginia 22151

TABLE OF CONTENTS

ANALYSIS OF CHARRING ABLATION WITH DESCRIPTION OF ASSOCIATED COMPUTING PROGRAM

Fred W. Matting

Ames Research Center

SUMMARY

A general method is presented for solving the problem of heat-shield response in the stagnation region of a charring type ablator. The analysis is actually for the stagnation point of an axisymmetric blunt body, but it is a valid approximate method for calculations in the stagnation region of any arbitrary blunt body. The analysis is applicable to wind-tunnel or flight conditions, and the heat loadings are either arbitrarily assigned or they are calculated concurrently with the heat-shield response. Surface heating (or cooling) mechanisms accounted for are those due to convection, radiation, homogeneous combustion, heterogeneous combustion, surface material removal by means other than combustion (includes erosion), and sublimation. Physical and thermodynamic properties of the ablating material are arbitrarily assigned so that calculations can be made for various materials.

A typical application of the analysis is given as an illustration. The analysis is machine programmed for numerical solutions using a finite difference scheme, and a family of computing programs is used. These programs are described and instructions are provided for using them. The programs can be obtained from COSMIC, University of Georgia, Athens, Georgia, 30601.

INTRODUCTION

Heat shields of the charring ablator type are in general use for frontal or stagnation region protection of current space vehicles. The charring ablator system has proven to be quite successful, at least up to entry speeds corresponding to lunar returns. A considerable amount of performance data on various heat-shield materials has been and is being obtained in the laboratory, particularly in arc-jet wind tunnels. However, laboratory experiments cannot duplicate all the changing conditions encountered in entry flights. Thus analytical methods are needed for predicting heat-shield performance, and to evaluate the accuracy of the predictions, calculated results must be compared with laboratory data for any given heat-shield material. There are approximations in the analysis presented in this report, and there are some uncertainties in the effective physical and thermodynamic properties of materials considered. (As an example, the thermal conductivity of some chars, which is temperature dependent, may exhibit hysteresis depending on the maximum temperature to which the char has been exposed.) When satisfactory checks between calculations and a range of experiments are obtained, we can assume that the

material properties are being adequately represented, and we have confidence in making calculations for flights.

A general method is presented here for determining the material response of a charring ablator in the stagnation region of a blunt body. The analysis has been formed for an axisymmetric stagnation point, but it is essentially valid in the stagnation region of any blunt body. The analysis is applicable to both wind tunnel and flight, and in either case the heat loading can be calculated concurrently with the heat-shield response or arbitrarily assigned. The heat shield can have an assigned finite depth, or a calculation using a semi-infinite depth can be made. Surface energy transfer mechanisms accounted for include those due to convection, radiation, homogeneous combustion, heterogeneous combustion, surface material removal by means other than combustion (includes erosion), and sublimation. Internally, the material receives (or loses) sensible heat, and it pyrolyzes (in a zone) from the original virgin plastic to (finally) pure char.

An attempt has been made to represent the charring ablation problem mathematically in an accurate but simple manner. Some parts of the analysis are similar to the analysis of surface ablation in reference 1, but many of the basic mechanisms require a different analysis. The analysis has been machine programmed for numerical solutions. External conditions, material properties, and various calculation options can be read in arbitrarily, and a family of computing programs is used to handle the various types of cases. The results of a typical example are presented to illustrate the various calculations that can be made. The principal features of the computing programs are described, and instructions are provided for use of the programs.

ANALYSIS AND METHOD OF SOLUTION

Basic Approach and Approximations

The analysis is concerned with the problem of charring type ablation that occurs in the stagnation region of a blunt body. The ablating material can be considered to be either very thick (semi-infinite) or of finite depth. The type of ablation studied includes pyrolysis or degradation inside the material. It also involves surface removal of material by heterogeneous combustion, by erosion or surface chemical reaction other than combustion, and by sublimation. Heat liberated by chemical reactions between the gases expelled and the external gas is also taken into account.

The external heat loading (convective and radiative) on the ablator can be put into the calculations in two ways: either arbitrarily programmed as a function of time, or calculated concurrently with the heat-shield response. For wind-tunnel cases, the loadings, either programmed as input or calculated, are usually essentially constant. For flight cases, the loadings usually vary greatly with time. Their calculation involves the simultaneous solution of trajectory equations with the ablation equations.

The ablation response analysis is strictly set up for the stagnation point of an axisymmetric blunt body. The analysis is also used as a good approximation to calculate the heat-shield response in the stagnation region of an arbitrary blunt body. The external heat loading at the point for which the response calculations are made must be known (or calculated). The analysis has also been used for response calculations at points far from the stagnation region. This use is quite approximate, but it is not necessarily unreasonable when the heat loading at such points is relatively small. Since the analysis is essentially one-dimensional, the approximate use assumes that lateral heat transfer is negligible compared to heat transfer normal to the surface.

As will be seen, the principal equation to be solved is a time-dependent energy equation that describes an energy balance in the interior of the material. A number of auxiliary equations are used to evaluate terms within it. The energy equation is a partial differential equation of parabolic type with independent variables, time, t, and depth in the material, y. Boundary conditions are determined by surface energy balance equations, and initial conditions must be supplied. The energy equation is solved numerically by finite differences.

Conservation Equations

The analysis is essentially a time-dependent energy balance along the stagnation center line of an axisymmetric blunt body. The one-dimensional coordinate system used is shown in sketch (a). The basic equations to be solved are the conservation equations for energy and mass, written in a simplified form that is valid in the stagnation region. The densities of virgin material and pure char, respectively ρ_p and ρ_{ch}, are considered constant. The conservation equations used are:

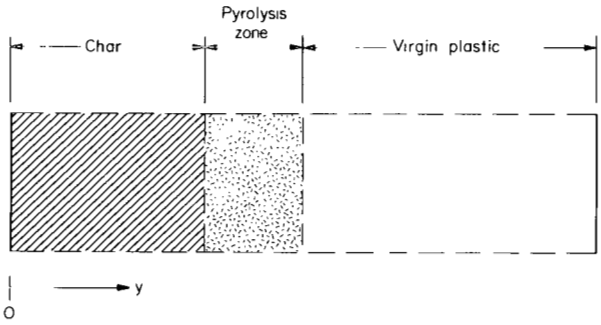

Sketch (a).- Coordinates.

Energy Equation

$$\left(\rho_s c_s + \rho_g c_{pg}\right) \frac{\partial T}{\partial t} + \left(\rho_s c_s \overline{v}_s - \dot{m}_g c_{pg}\right) \frac{\partial T}{\partial y} = \frac{\partial}{\partial y}\left(\overline{\overline{K}}_s \frac{\partial T}{\partial y}\right) + \dot{w}_g h_{sr} \qquad (1)$$

where

$$\overline{v}_s = \overline{v}_{s\,comb} + \overline{v}_{s\,ero} + \overline{v}_{s\,sub}$$

$$= \overline{v}_s(t) \quad \text{(i.e., independent of } y) \qquad (2)$$

$\dot{w}_g$ rate of production of pyrolysis gases per unit space volume, g/cm^3sec (≥ 0)

$\dot{m}_g$ rate of flow of pyrolysis gases past a point, taken as an absolute valued quantity, g/cm^2sec

h_{sr} energy released by the pyrolysis reaction, cal/g of gas produced; $h_{sr} < 0$ for endothermic reactions. This can be described as a function of temperature, but it can often be conveniently approximated as a constant (see appendix A).

Equation (1) is considered to be a reasonable approximation. The thermal conductivity of gaseous material is neglected (or can be considered as lumped into the $\bar{\bar{K}}_s$ term). Also neglected are viscous dissipation and compression work. Secondary chemical reactions involving the pyrolysis gases as they flow through the solid material are not specifically treated. Secondary gaseous reactions, if known along with their rates, can be accounted for approximately by selection of the temperature enthalpy variation of the pyrolysis gases.

Continuity Equation

Pyrolysis Gases

$$\frac{\partial \rho_g}{\partial t} - \frac{\partial \dot{m}_g}{\partial y} = \dot{w}_g \tag{3a}$$

Solid Material

$$\frac{\partial \rho_s}{\partial t} + \frac{\partial}{\partial y}(\rho_s \bar{v}_s) = \frac{D\rho_s}{Dt} = -\dot{w}_g \tag{3b}$$

where

$$\dot{w}_g = K(\rho_s - \rho_{ch})^n \tag{4}$$

The order of the pyrolysis reaction is n, and

$$K = S_p\, e^{-\frac{\theta_p}{T}} \tag{5}$$

is the Arrhenius formula for the reaction rate. The procedure will be to solve continuity equation (3b) for ρ_s and substitute the solution into the energy equation (1).

Solution of the Continuity Equation

We combine equations (3b) and (4) and have

$$\frac{D\rho_s}{Dt} = -K(\rho_s - \rho_{ch})^n = \frac{D}{Dt}(\rho_s - \rho_{ch}) \tag{6}$$

where $D\rho_s/Dt$ is a substantial derivative (i.e., it follows a certain small mass of the solid material).

Let

$$J = \frac{\rho_s - \rho_{ch}}{\rho_p - \rho_{ch}} \tag{7}$$

where $1 - J$ is the degree of degradation. Then

$$\frac{DJ}{Dt} = -(\rho_p - \rho_{ch})^{n-1} K J^n \tag{8}$$

with the (usual) initial condition $J_i(t_i) = 1$. In the integration of equation (8), we define:

$$z = \int_{t_i}^{t} K \, dt_1 \tag{9}$$

Equation (8) has the solutions:

$$J = \left[1 + (n - 1)(\rho_p - \rho_{ch})^{n-1} z\right]^{\frac{1}{1-n}} \quad \text{for} \quad n \neq 1 \tag{10a}$$

$$J = e^{-z} \quad \text{for} \quad n = 1 \tag{10b}$$

With the inversion of equation (7),

$$\rho_s = \rho_{ch} + (\rho_p - \rho_{ch}) J(y, t) \tag{11}$$

The type of asymptote for J expected indicates that one should expect $n \geq 1$. In any case, in the computing program, J is not allowed to become negative.

As noted above $D\rho_s/Dt$ is a substantial derivative and it refers to a specific location in the material:

$$y = y(y_i, t) \text{ which is } y = y_i + \int_{t_i}^{t} \bar{v}_s \, dt_1$$

$$K = K(T) \text{ and } T = T(y, t)$$

$$K = K\{T[y(y_i, t), t]\}$$

$$K = K\left[T\left(y_i + \int_{t_i}^{t} \bar{v}_s \, dt_1, t\right)\right]$$

This evaluation of K is used (in principle) in equation (9), the integral for z. The solution for ρ_s thus depends on the past history of a point in the material. When ρ_s is determined, $\dot{w}_g$ can be evaluated from equation (4) for substitution in the energy equation (1).

In the numerical computing program, z (eq. (9)) is obtained by a procedure that is equivalent to the equations developed above. Thus,

$$\Delta X = X - X_{-1}$$

The subscript, -1, refers to the previous time line; and X and X_{-1} represent total surface recession corresponding to the current and previous time lines, respectively. (Equation (59) is used to calculate X; see Surface Recession.) In the finite differencing scheme, the array, $y(M)$, is used where M is the spatial grid point number in the spatial finite differencing. A new array is needed for following the time history of specific points in the material:

$$\overline{y}_{-1}(M) = y(M) + \Delta X$$

where $\overline{y}_{-1}(M)$ for the previous time line and $y(M)$ for the current time line represent the same point in the material. From the previous time line we have saved the arrays $T_{-1}(M)$ and $z_{-1}(M)$ (which are spaced according to the $y(M)$ array). We interpolate against $\overline{y}_{-1}(M)$ to obtain the $\overline{T}_{-1}(M)$ and $\overline{z}_{-1}(M)$ arrays. We use equation (5) with the argument $\overline{T}_{-1}(M)$ to obtain the $\overline{K}_{-1}(M)$ array. We then obtain

$$z(M) = 0.5[K(M) + \overline{K}_{-1}(M)]\Delta t + \overline{z}_{-1}(M) \tag{12}$$

where Δt is the finite time increment between the previous and current time lines. This is the numerical solution to the integral in equation (9); the z values thus obtained are used in equation (10). (It will be seen later that $T(M)$ and hence $K(M)$ are known at this point in the calculation procedure.)

Physical Properties of Solid Material

Physical properties of the solid material will, in general, depend on temperature and on the extent of degradation. We need the specific heat and thermal conductivity of both the virgin plastic and pure char as functions of temperature. Data for partially degraded material would also be desirable, but in its absence we assume a linear relationship with density as below.

$$c_s = c_{ch} + (c_p - c_{ch})\left(\frac{\rho_s - \rho_{ch}}{\rho_p - \rho_{ch}}\right) \tag{13a}$$

Thus:

$$c_s = c_{ch} + (c_p - c_{ch})J \tag{13b}$$

Equation (13) is the general formula for the physical properties of the solid material. It is not perfectly consistent with a volumetric model sketched in the next section, but it is considered to be within the framework of approximations used.

The formula assumed for thermal conductivity is somewhat exceptional; it is of the same form as equation (13), but it is also modified by an empirical multiplying factor.

$$\overline{\overline{K}}_s = [\overline{\overline{K}}_{ch} + (\overline{\overline{K}}_p - \overline{\overline{K}}_{ch})J][1 - 4(1 - C_J)J(1 - J) \tag{14}$$

The modifying multiplier in equation (14) changes the thermal conductivity in the pyrolysis zone ($0 < J < 1$). The maximum modification (at $J = 0.5$) by C_J, a read-in quantity, is generally a reduction to account for the reduced conductivity in the pyrolysis zone of some materials. (Values of C_J of 0.6 to 1.0 have been used in matching wind-tunnel data.) If no modification is wanted, C_J is assigned a value of unity.

For some materials a reduction in thermal conductivity may be accompanied by a similar reduction in density in the pyrolysis zone, but since the overall effect on the calculations is small, it is neglected in the analysis. (The computer programs could be modified to include it.) Reduced thermal conductivity across a narrow zone can have an effect because it influences the heat transfer across that zone.

Physical properties are computed by a material properties subprogram for this purpose. Data may be either tabular or in equation form as inputs to the subprogram.

Rate of Flow of Pyrolysis Gases

The rate of flow of pyrolysis gases past a station, $\dot{m}_g$, is a term in the energy equation (1). This can be evaluated by summing up the rate of gas production between a station and the interior when one neglects the small change in gas stored in the interior. Equivalently, one can evaluate the rate of mass loss of solid material between a station and the interior to give the rate of gas production. This latter is the method that is used. The calculation requires knowledge of the surface recession rate. This rate (the velocity of solid material in the coordinate system, $\overline{v}_s$) is obtained from equation (2). The components in equation (2), which are summed up, are obtained from surface calculations which are described below in the section, Surface Recession Velocity.

The gas density, ρ_g, in equation (1), is actually the weight of gas in a unit volume of space (with a portion of the unit volume taken up by solid material). The gas is assumed to be at the local temperature of the solid material and at the external pressure, p_{s_2}. Using the perfect gas law we have

$$\rho_g = \frac{p_{s_2} \overline{\overline{v}}_g M_g}{R_g T} \tag{15}$$

where R_g is the universal gas constant and $\overline{\overline{v}}_g$ is the volume actually occupied by the gas in a unit spatial volume. Using our simple model for the density of the solid material, we have

$$\rho_s = \rho_{ch}(1 - J) + \rho_p J \tag{11}$$

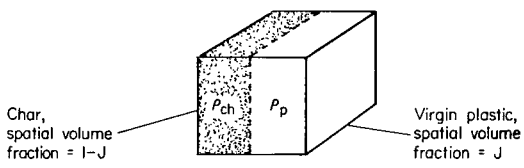

Sketch (b).- Volume fraction.

which can be visualized in a simplified way as shown in sketch (b). We need the volume fraction actually occupied

by the solid part of the char, which is, in turn, a fraction of the spatial volume occupied by the char.

$$\bar{\bar{v}}_{cha} = \frac{\rho_{ch}(1 - J)}{\rho_{cha}} = \frac{\text{Volume of solid char material}}{\text{Total volume}} \tag{16}$$

Then

$$\bar{\bar{v}}_g = (1 - J) - \frac{\rho_{ch}(1 - J)}{\rho_{cha}} \tag{17a}$$

$$\bar{\bar{v}}_g = (1 - J)\left(\frac{\rho_{cha} - \rho_{ch}}{\rho_{cha}}\right) \tag{17b}$$

Equation (17b) contains the porosity of the char:

$$Por = \frac{\rho_{cha} - \rho_{ch}}{\rho_{cha}} \tag{17c}$$

Equation (17b) is combined with equation (15) to give

$$\rho_g = \frac{p_{s_2} M_g}{R_g T}(1 - J)\left(\frac{\rho_{cha} - \rho_{ch}}{\rho_{cha}}\right) \tag{18}$$

where ρ_g is the mass of gas per unit spatial volume.

As noted above, the term $\dot{m}_g$ in equation (1) is the mass rate of gas flow past a given station. When the small change in gas stored in a control volume is neglected, the gas flow rate past a station is approximately the gas production rate that occurs at all depths that are deeper in the material. In sketch (c) the dotted line represents the control volume, and the solid and gaseous material is flowing from right to left. The term $\dot{m}_g$ is a positive quantity. Continuity for the control volume with the semi-infinite formulation is:

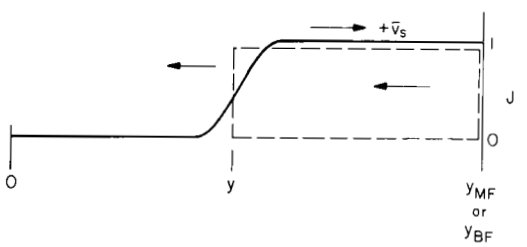

Sketch (c).- Control volume.

$$\dot{m}_g(y, t) + \bar{v}_s(t)\left[\rho_s(y_{MF}, t) - \rho_s(y, t)\right] = -\frac{\partial}{\partial t}\int_y^{y_{MF}} \rho_s \, dy_1 \tag{19}$$

Equation (19), then, neglects the rate of change of the amount of gas stored in the control volume, which must be small. The value of y_{MF} is constant as it is fixed in the spatial coordinate system. It is also large enough that no degradation reaches it, so it can represent infinite depth.

$$\dot{m}_g(y, t) = (\rho_p - \rho_{ch})\left\{\overline{v}_s(t)[J(y, t) - J(y_{MF}, t)] - \frac{\partial}{\partial t}\int_y^{y_{MF}} J(y_1, t)dy_1\right\} \tag{20}$$

The finite depth formulation is similar but is slightly different in form. In place of equations (19) and (20) we have

$$\dot{m}_g(y, t) - \overline{v}_s(t)\rho_s(y, t) = -\frac{\partial}{\partial t}\int_y^{y_{BF}} \rho_s \, dy_1 \tag{21a}$$

$$\dot{m}_g(y, t) = (\rho_p - \rho_{ch})\left[\overline{v}_s(t)J(y, t) - \frac{\partial}{\partial t}\int_y^{y_{BF}} J(y_1, t)dy_1\right] \tag{21b}$$

The limit, y_{BF}, is not fixed in the coordinate system; it is the depth of the back surface of the material. It shrinks at the rate $|\overline{v}_s|$. Equations (20) and (21) are actually equivalent. As evaluated by the computing program, the integral in equation (20) or (21) is calculated for the current and the previous time lines, and the partial derivative with time is approximated as a difference quotient with denominator, Δt.

Surface Recession Velocity

The surface recession velocity, $\overline{v}_s$, appears in equations (20) and (21) as well as in equation (1). For $\overline{v}_s$, we can rewrite equation (2) as

$$\overline{v}_s = -\frac{1}{\rho_s}(\dot{m}_{scomb} + \dot{m}_{sero} + \dot{m}_{ssub}) \tag{22}$$

where the $\dot{m}$'s are ≥ 0. With a charring ablator, there is essentially no surface recession prior to the beginning of pyrolysis. With the onset of pyrolysis (which proceeds back from the front surface), a charred front face is quickly obtained. Thus, we write and use for $\overline{v}_s$:

$$\overline{v}_s = -\frac{1}{\rho_{ch}}(\dot{m}_{chcomb} + \dot{m}_{chero} + \dot{m}_{chsub}) \tag{23}$$

We now evaluate $\dot{m}_{chcomb}$, $\dot{m}_{chero}$, and $\dot{m}_{chsub}$. (These are computed in the material properties subprogram.)

Char combustion rate-In calculating the char combustion rate, $\dot{m}_{chcomb}$, we first evaluate the amount of oxygen that can diffuse to the char surface to perform combustion. In the model chosen, it is assumed that the pyrolysis gases burn, and have first claim on the available oxygen, leaving a lesser amount available for heterogeneous combustion. It is assumed that the homogeneous burning occurs at a flame front near the outer edge of the boundary layer. The maximum air flow per unit area is

$$\dot{m}_{\substack{air \\ max}} = (\rho_{air} v_{air})_{max} = 0.1 D V_\infty \tag{24a}$$

From boundary-layer theory we have

$$\dot{m}_{\substack{air \\ calc}} = (\rho_{air} v_{air})_{\substack{e \\ calc}} = 0.462 \bar{\phi} \sqrt{\frac{p_{t_2}}{R}} \tag{24b}$$

where $\bar{\phi}$ is a dimensionless stream function that normally takes the value, unity (see appendix B, eq. (B7)). For gases other than air, and for off-stagnation approximate calculations, $\bar{\phi}$ may be assigned values other than unity. The air available for oxygen diffusion is taken to be

$$\dot{m}_{air} = (\rho_{air} v_{air})_e = \text{lesser of the values from equations (24)} \tag{25}$$

The available oxygen is

$$\dot{m}_{ox} = \dot{m}_{air} C_{ox} \tag{26}$$

where C_{ox} is the mass fraction of oxygen in the ambient gas. The oxygen theoretically used in the homogeneous combustion is:

$$\dot{m}_{\substack{ox \\ theo}} = \dot{m}_{gw} E_2 \tag{27}$$

where $\dot{m}_{gw} = \dot{m}_g(0, t)$ is the rate of pyrolysis gas expulsion and E_2 is the stoichiometric ratio of oxygen to pyrolysis gas for the reaction assumed to take place. The excess oxygen is

$$\dot{m}_{\substack{ox \\ ex}} = \dot{m}_{ox} - \dot{m}_{\substack{ox \\ theo}} \tag{28}$$

If $\dot{m}_{\substack{ox \\ ex}} < 0$, there is no excess oxygen and not all the pyrolysis gases are burned. The heat liberated by combustion of the pyrolysis gases is proportionately reduced, and according to our model, there is then no heterogeneous combustion. If

$$\dot{m}_{\substack{ox \\ ex}} < 0 \tag{29a}$$

then we use

$$\dot{m}_{\substack{ox \\ ex}} = 0 \tag{29b}$$

in all subsequent calculations. For the concentration of oxygen by weight available for heterogeneous combustion, we can write

$$C_{oxf} = C_{ox}\left(\frac{\dot{m}_{\substack{ox \\ ex}}}{\dot{m}_{ox}}\right) \tag{30}$$

For heterogeneous combustion, oxygen must diffuse to the wall, giving a concentration at the wall, C_{oxw}. The kinetic reaction rate depends on C_{oxw}. Since there is no accumulation or depletion of oxygen in a quasi-steady state process, the diffusion rate and the kinetic rate of consumption of oxygen must be equal.

For the oxygen diffusion rate, we use the Lewis analogy (with Le = 1); (see ref. 1). This states that the ratio of the rate of diffusion of a species to its concentration potential equals the ratio of the continuum convective heat-transfer rate (corrected by a blowing factor) to the enthalpy potential.

$$\frac{\dot{m}_{oxd}}{C_{oxf} - C_{oxw}} = \frac{\psi q_{oc}}{\Delta h} = \frac{\psi q_{oc}}{\left[\frac{V^2}{0.00836} - \overline{c}_p T_w\right]} \tag{31}$$

where the continuum convective heat-transfer rate, q_{oc}, the blowing factor, ψ, and the enthalpy velocity V, are evaluated in the section, Surface Heat Transfer. With the evaluation for q_{oc} (eq. (62)), and neglecting any vorticity correction on q_{oc}, one can write

$$\frac{\dot{m}_{oxd}}{C_{oxf} - C_{oxw}} = 0.00836\psi A_4 \sqrt{\frac{D}{R}}\, V^{1.15} = K_d \tag{32}$$

$$\dot{m}_{oxd} = K_d(C_{oxf} - C_{oxw}) \tag{33}$$

where K_d depends on external conditions, nose radius, and the rate of expulsion of pyrolysis gases. The theoretical maximum oxygen diffusion rate occurs when the wall concentration is zero.

$$\dot{m}_{\substack{oxd \\ max}} = K_d C_{oxf} \tag{34}$$

For the reaction rate of oxygen consumption in the surface combustion we use an Arrhenius type of rate constant.

$$K_{ox} = K_r\, e^{-\frac{C_E}{T_w}} \tag{35}$$

Then for a reaction of order j we have

$$\dot{m}_{oxr} = K_r\left[\rho_{\substack{air \\ w}} C_{oxw}\right]^j e^{-\frac{C_E}{T_w}} \tag{36}$$

$$= K_r\left(\frac{p_{t_2} C_{oxw}}{R_{air} T_w}\right)^j e^{-\frac{C_E}{T_w}} \tag{37}$$

where R_{air}, the gas constant for air (or other external gas), is approximated as independent of the oxygen concentration. Upon combining constants:

$$K_1 = \frac{K_r}{R_{air}^j} \tag{38}$$

where K_1 is the constant read into the computing program. Then

$$\dot{m}_{oxr} = K_1\left(\frac{p_{t_2} C_{oxw}}{T_w}\right)^j e^{-\frac{C_E}{T_w}} \tag{39}$$

The maximum theoretical reaction rate would occur with an oxygen mass fraction of unity, so we define

$$K_{re} = K_1\left(\frac{p_{t_2}}{T_w}\right)^j e^{-\frac{C_E}{T_w}} \tag{40}$$

(Actually C_{oxw} cannot exceed C_{oxf}.) Then

$$\dot{m}_{oxr} = K_{re}(C_{oxw})^j \tag{41}$$

With the quasi-steady state assumed,

$$\dot{m}_{ox} = \dot{m}_{oxd} = \dot{m}_{oxr} \tag{42}$$

With the substitution of equation (42) into equations (33) and (41), we have two equations in two unknowns, $\dot{m}_{ox}$ and C_{oxw}, that can be solved. In computations, one generally assumes the combustion reaction to be of half order ($j = 0.5$). (This should be the case for the combustion of carbon with undissociated oxygen to carbon monoxide, $C + (1/2)O_2 \rightarrow CO$.) In two typical material properties subprograms, $j = 0.5$ is "built in"; in a third subprogram, j is an arbitrary read-in quantity (see appendix C). Finally, the rate of oxygen consumption is converted into char combustion

$$\dot{m}_{chcomb} = \frac{\dot{m}_{ox} C_{kdb}}{C_x} \tag{43}$$

where C_{kdb} is the reciprocal of the fraction of char that is carbon, and the noncombustible fraction of the char is assumed either to melt off or blow off. The quantity, C_x, is the stoichiometric ratio of oxygen to carbon in the reaction. With the usual assumption of combustion of carbon to CO, C_x is 4/3. For the theoretical maximum rate of char combustion by diffusion we have from equations (34) and (43)

$$\dot{m}_{\substack{chcomb \\ d\ max}} = \frac{\dot{m}_{\substack{oxd \\ max}} C_{kdb}}{C_x} \tag{44}$$

From equations (40), (41), and (43), the maximum rate of char combustion, as determined by the reaction rate and the available oxygen, is

$$\dot{m}_{\substack{chcomb \\ r\ max}} = \frac{K_{re}(C_{oxf})^{j}C_{kdb}}{C_x} \tag{45}$$

The rate of char combustion, $\dot{m}_{chcomb}$, cannot exceed either $\dot{m}_{\substack{chcomb \\ d\ max}}$ or $\dot{m}_{\substack{chcomb \\ r\ max}}$. The quantity, $\dot{m}_{\substack{chcomb \\ d\ max}}$, would be the rate if the reaction rate were infinite, and $\dot{m}_{\substack{chcomb \\ r\ max}}$ would be the rate if diffusion were instantaneous. These quantities are of interest, because the approach of $\dot{m}_{chcomb}$ to one value or the other denotes "diffusion control" or "reaction rate control" of the char combustion rate.

Char erosion rate-For the char consumption rate by other than combustion or sublimation, we do not fully understand the mechanisms involved, and we use empirical calculations. We call this consumption rate erosion, $\dot{m}_{chero}$, although there may be chemical reactions (and energies) involved. The empirical calculations should be related to wind-tunnel experiments in inert gases and also in air for a given material. The erosion rate will vary considerably for different materials because of the variation of density and structural integrity of the char produced.

An equation that can be used for erosion is of the Arrhenius type:

$$\dot{m}_{chero} = \rho_{sw}\alpha_1\left(\frac{p_{t_2}}{T_w}\right)^{m} e^{-\frac{\alpha_2}{T_w}}(1 - K_2) \tag{46a}$$

Another type of equation that is based on experience at Ames Research Center has been used for several materials (e.g., for phenolic nylon):

$$\dot{m}_{chero} = \rho_{sw}[\alpha_1 + \alpha_2 T_w + \alpha_3(T_w - \alpha_4)^{m}](1 - K_2) \tag{46b}$$

Equation (46) (of whatever type) is in the material properties subprogram for a given material. The constants α_i and m can be read in using open symbols available (see appendix C, Input Data), or the constants can be written numerically into the material properties subprogram. Threshold temperatures can also be used, above which the constants change values (so that wind-tunnel data can be fit very closely).

Experiments in inert gases and in air have indicated that for some materials, the surface recession due to erosion and combustion may not be completely additive (or the one may partly suppress the other). The factor $(1 - K_2)$ in equations (46) is used to account for this empirically, where $0 \le K_2 < 1$ is a read-in quantity. As examples, for the Apollo type heat

shield material, $K_2 = 0.6$ has been used, while for high-density phenolic nylon, $K_2 = 0$ has been used.

It is possible to write more complicated expressions for erosion than the examples in equation (46) by postulating several failure mechanisms. For example, a dependence on external pressure gradient would include a term that would be a function of p_{t_2}/R.

Sublimation rate-The calculation of the mass loss rate by sublimation, $\dot{m}_{chsub}$, requires a bridging between the free-molecule rate and the diffusion controlled rate. This is developed in appendix C of reference 1.

The free-molecule rate of sublimation in a vacuum is calculated by the Langmuir equation (refs. 1 and 2):

$$\dot{m}_{chsFM} = A_{cv} p_{ve} C_{dy} C_{kdb} \sqrt{\frac{M_{cv}}{2\pi R_g T_w}} \tag{47}$$

where C_{dy} is the pressure of a standard atmosphere in dynes/cm^2, so that the vapor pressure, p_{ve}, is in atmospheres. The constant, C_{kdb}, converts the carbon sublimation rate to that of the entire char. The assumption is that the carbon rate controls, and the other material in the char either melts off or is blown off. With evaluation of constants we have

$$\dot{m}_{chsFM} = 44.37 A_{cv} p_{ve} C_{kdb} \sqrt{\frac{M_{cv}}{T_w}} \tag{48}$$

The equilibrium vapor pressure, p_{ve}, is evaluated as

$$p_{ve} = e^{E_8 - \frac{E_{19}}{T_w}} \tag{49}$$

For the sublimation rate with diffusion control, we use the equilibrium vapor pressure, p_{ve}, but consider that it can be modified to a value, p_{vm}, by homogeneous chemical reactions. As in reference 1, this modification is approximated as

$$\frac{p_{t_2}}{p_{vm}} = \left(\frac{p_{t_2}}{p_{ve}}\right)^{E_7} \tag{50}$$

where $E_7 = 1$ represents no modification (which is the usual case). We define

$$p = \frac{p_{t_2}}{p_{vm}} - 1 = \left(\frac{p_{t_2}}{p_{ve}}\right)^{E_7} - 1 \tag{51}$$

and we use the Lewis analogy equation as in reference 1 for the rate of mass diffusion (see also refs. 3 and 4).

$$\dot{m}_{chsd} = \frac{0.00836\psi q_{oc} C_{kdb}}{p\left(\frac{M_p}{\bar{M}_{cv}}\right)[V^2 - 0.00836\bar{c}_p T_w]} \tag{52}$$

where C_{kdb} converts from the carbon diffusion rate to the rate of entire char consumed, and where M_p is the molecular weight of the gaseous products (after heterogeneous combustion). It is assumed that this is essentially the gas through which the carbon vapor must diffuse.

For the mass loss rate by sublimation we have finally (see ref. 1):

$$\frac{1}{\dot{m}_{chsub}} = \frac{1}{\dot{m}_{chsFM}} + \frac{1}{\dot{m}_{chsd}} \tag{53}$$

In the development above we have lumped all components of the char together, and we have assumed that the carbon sublimation rate controls the rate of consumption of char. The other components of the char may affect the constants used, such as equilibrium vapor pressure, p_{ve}, and accommodation coefficient, A_{cv}, but as a reasonable approximation, the constants for carbon are probably satisfactory for most chars. Typical values used for char constants are: $E_8 = 22.3$, $E_{19} = 91{,}600$, $A_{cv} = 1.0$, $M_{cv} = 33$, and $M_p = 15$. Sublimation, for many conditions, is a small factor in the ablation process. It can become important and even dominant, however, for very high speed flights such as from planetary returns.

Quantities Required for Subsequent Calculations

Total pressure-For the total pressure, p_{t_2} (atmospheres), for flight calculations we use a hypersonic approximation, twice the free-stream dynamic pressure with a correction factor (ref. 1)

$$p_{t_2} = \frac{A_1 DV^2}{101.3} \tag{54}$$

where a typical value for A_1 is 0.95, and the number, 101.3, accounts for the units in the equation. For the wind-tunnel case, p_{t_2} is a read-in quantity. Also

$$p_{s_2} = 1.013\times10^6 p_{t_2} \tag{55}$$

where p_{s_2} is the pressure in dynes/cm^2. For the arbitrary heating rate computing programs, p_{t_2} as a function of time is read into the program. For off-stagnation approximate calculations, A_1 should be adjusted so that p_{t_2} in equation (54) becomes a local pressure, p_w. This also applies to arbitrary heating rate calculations because, in these cases, equation (54) is inverted to obtain the free-stream density, D, from the programmed pressure, p_{t_2} or p_w.

Enthalpy velocity-In place of using the enthalpy of the external gas for surface heat-transfer calculations, it is convenient to use an "enthalpy velocity," in km/sec, which is defined as (ref. 1):

$$V^2 = 0.00836h_{st} \tag{56a}$$

$$V = 0.0915\sqrt{h_{st}} \tag{56b}$$

where h_{st} is in cal/g.

Specific heat of external gas-It is convenient to use an average specific heat for the external gas (as in ref. 1). This is defined as

$$\overline{c}_p = \frac{1}{T}\int_o^T c_p \, dT_1 \tag{57a}$$

We use the evaluation

$$\overline{c}_p = E_{10} + E_3 T_w \tag{57b}$$

where E_{10} and E_3 are normally constant read-in values. If a higher order representation is desired, E_{10} and E_3 can be made functions of temperature in the material properties subprogram. Values of $E_3 = 0.84\times10^{-4}$ and $E_{10} = 0.1267$ have been used for air at flight conditions.

Surface recession-The surface recession, χ, is a quantity of interest, and it is also used in evaluating other quantities.

$$\dot{\chi} = |\overline{v}_s| \tag{58}$$

$$\chi = \int_{t_i}^{t} \dot{\chi} \, dt_1 + \chi_i \tag{59}$$

Nose radius-The effective nose radius, R, is needed for the calculation of the convective continuum heat-transfer rate, q_{oc}. The R is calculated as a quantity that has an empirical variation with surface recession (as in ref. 1).

$$R = R_i[1 + E_{17}\chi^2 + c_1(e^{c_2\chi} - 1)] \tag{60}$$

The constants should be evaluated experimentally if possible; otherwise, a recession shape geometry must be assumed. For a negligible shape change, the constants have the value zero. In the arbitrary heating-rate computing programs, the R, as a function of time, is programmed as an input. For approximate calculations off the stagnation point, the value of R may be a fictitious effective value.

Tumbling factor-Tumbling or oscillation in flight will reduce both the convective and radiative heat transfer into the point on the body that is

taken as the nominal stagnation point. The quantity, $\overline{K}_{tu}$, is used as a multiplying factor on the heat-transfer rates. It is evaluated empirically (as in ref. 1) as

$$\overline{K}_{tu} = \overline{K} + (1 - \overline{K})\left[1 - e^{-\left(\frac{x}{\chi_1}\right)^{E_{16}}}\right] \tag{61}$$

where $\overline{K}$ is the fractional time that the point on the body (nominal stagnation point) is initially exposed to approximately stagnation conditions, and χ_1 and E_{16} are values selected to give a realistic damping to the oscillation during an entry flight. For the entry of a small body that tumbles initially, but achieves stability, the values have been used: $\overline{K} = 0.25$, $\chi_1 = R/10$ cm, and $E_{16} = 1.0$. For a nontumbling body, $\overline{K}$ is unity, giving a $\overline{K}_{tu}$ of unity. For the arbitrary heating-rate computing programs, $\overline{K}_{tu}$ is not used, but it is considered to be "built in" to the assigned heating rates.

Surface Convective Heat-Transfer Rate

The equations listed below are identical with equations (15) through (25) as developed in reference 1.

These equations are not used in the arbitrary heating-rate computing programs; for those cases we use only equations (72) (inverted) and (73).

In the calculated heating-rate computing programs, for laminar continuum flow, the surface convective heat transfer is evaluated as (refs. 1 and 5):

$$q_{oc} = A_4\sqrt{\frac{D}{R}}\,V^{1.15}[V^2 - 0.00836\overline{c}_p T_w]\left(1 + \frac{C_6}{\sqrt{DVR}}\right) \tag{62}$$

where A_4 is a constant, and C_6 is a (generally small, $0 \le C_6 < 0.2$) vorticity correction. (A_4 and C_6 are not used with the arbitrary heating-rate computing programs.) For wind-tunnel tests, A_4 should be evaluated with a calorimeter; the value of A_4 for earth entries is approximately 1.1. With a blowing correction, we have

$$q_{\psi c} = \psi q_{oc} \tag{63}$$

where ψ is evaluated in the section, Blowing Factor.

For rarefied conditions, the evaluation of the surface convection rate in free-molecule flow is needed. We use the Newtonian type approximation (refs. 1 and 6):

$$q_{FM} = \frac{A_{cq}DV_\infty}{0.0836}\,[V^2 - 0.00836\overline{c}_p T_w] \tag{64}$$

The accommodation coefficient, A_{cq}, is ≤ 1. If unknown, it is usually assigned the value unity (at or near the stagnation point). In the transition regime between free-molecule and continuum flow, we use a relationship that gives a value of convective heat transfer that is bridged between the free-molecule and the continuum evaluations (ref. 1).

$$q_{\psi w} = q_{\psi c}\left[1 - e^{-\left(\frac{q_{FM}}{q_{\psi c}}\right)}\right] \tag{65}$$

Equation (65) is used for all regimes; it automatically gives the correct free-molecule and continuum asymptotes. When the tumbling correction is applied, the convective heat transfer at the front surface is evaluated as

$$q_w = q_{\psi w}\overline{K}_{tu} \tag{66}$$

In equations (62) to (66), all the convective heat-transfer rates that are actually needed are obtained. However, we can also calculate several additional related quantities. When there is no mass transfer ($\psi = 1$), equation (65) specializes to

$$q_{oo} = q_{oc}\left[1 - e^{-\left(\frac{q_{FM}}{q_{oc}}\right)}\right] \tag{67}$$

and equation (66) becomes

$$q_o = q_{oo}\overline{K}_{tu} \tag{68}$$

With mass transfer, we can define a modified ψ that operates on q_{oo} (instead of on q_{oc} as developed above). The modified blowing factor is defined as (ref. 1):

$$\overline{\psi} = \frac{q_{\psi w}}{q_{oo}} \tag{69a}$$

$$q_{\psi w} = \overline{\psi} q_{oo} \tag{69b}$$

Multiplying equation (69b) by $\overline{K}_{tu}$ and using equations (66) and (68) we have:

$$q_w = \overline{\psi} q_o \tag{70}$$

We substitute equations (63), (65), and (67) into (69a) to obtain an evaluation of $\overline{\psi}$.

$$\overline{\psi} = \frac{\psi\left[1 - e^{-\left(\frac{q_{FM}}{\psi q_{oc}}\right)}\right]}{1 - e^{-\left(\frac{q_{FM}}{q_{oc}}\right)}} \tag{71}$$

The development from equation (67) to (71) is an alternate form of convective heat-transfer analysis. It is entirely equivalent to the previous development in equations (65) and (66). The new quantities obtained, q_{oo}, q_o, and $\overline{\psi}$, are considered to be of conceptual interest. Both developments are calculated and the quantities obtained are read out by the computing programs.

Another quantity of interest that is calculated is the cold-wall convective heating rate, q_{ocw} (not in ref. 1). This has been defined to include the oscillation correction, so it is the heating rate that would be received by a cold front surface with no mass transfer occurring.

$$q_{ocw} = \frac{q_o V^2}{V^2 - 0.00836\overline{c}_p T_w} \tag{72}$$

For normal (nonrarefied) wind-tunnel conditions, the bridging relations between the free-molecule and continuum regimes are not needed; also there is no oscillation. We have then:

$$\overline{K}_{tu} = 1 \tag{73a}$$

$$\overline{\psi} = \psi \tag{73b}$$

$$q_o = q_{oc} \tag{73c}$$

$$q_w = \psi q_o = \psi q_{oc} \tag{73d}$$

The cold-wall convective heating rate is given by equation (72) for this case also.

When the arbitrary heating rate computing programs are used, the cold-wall convective heating rate, q_{ocw}, as a function of time, is programmed as an input. The oscillation correction and rarefaction effects are already entered. We invert equation (72) to solve for q_o, and we use equation (73) to solve for the front-face convective heating rate, q_w.

Blowing Factor

As noted in the preceding section, for the evaluation of the surface heat transfer by convection, it is necessary to know the blowing factor, ψ. This

is evaluated empirically in terms of the blowing parameter, B, which is defined below. The total mass loss rate of material is

$$\dot{m}_T(t) = \dot{m}_g(0, t) - \overline{v}_s(t)\rho_s(0, t) \tag{74a}$$

$$\dot{m}_T(t) = \dot{m}_g(0, t) + (\dot{m}_{chcomb} + \dot{m}_{chero} + \dot{m}_{chsub}) \frac{\rho_s(0, t)}{\rho_{ch}} \tag{74b}$$

We also calculate, as a quantity of interest, the total mass loss of material (per unit area) as:

$$M_T = \int_{t_i}^{t} \dot{m}_T \, dt_1 + M_{T_i} \tag{74c}$$

For the gaseous material that contributes to heat blockage one should add the oxygen that is consumed in heterogeneous combustion. The oxygen in the homogeneous combustion is not included because we are using a flame front model that considers the homogeneous combustion to occur at the outer edge of the boundary layer. For the blockage-contributing mass loss rate:

$$\dot{m}_c = \dot{m}_g(0, t) + \frac{1}{C_{kdb}} [\dot{m}_{chcomb}(1 + C_x) + A_3\dot{m}_{chero} + \dot{m}_{chsub}] \frac{\rho_s(0, t)}{\rho_{ch}} \tag{75}$$

Division by the factor C_{kdb} means that only the carbon in the char contributes to blockage. The material other than carbon is assumed to either melt off or be blown off as a solid. The constant, A_3, allows the option of selecting whether or not the eroded carbon contributes to blockage. When $A_3 = 1$, the eroded carbon is included; when $A_3 = 0$, the eroded carbon is not included. The latter is probably the usual case, where eroded material is removed in the form of solid particles. $A_3 = 0.5$ has also been used which means that half the eroded material is assumed to be gaseous. A value of $A_3 > 1$ can be used to represent removal of material by some chemical reaction other than combustion and release of the products in gaseous form. The blowing parameter is defined as

$$B = \dot{m}_c \frac{\Delta h}{q_{oc}} \tag{76a}$$

$$B = \dot{m}_c \sqrt{\frac{R}{D}} \frac{1}{0.00836A_4V^{1.15}} \tag{76b}$$

In going from equation (76a) to (76b), the vorticity correction in equation (62) is neglected.

The blowing factor, ψ, is approximated as a linear function of B (refs. 3, 4, 7) with a slope that depends on the molecular weight of the gaseous products, M_p (after heterogeneous combustion). The value of ψ is prevented from going negative with large B by arbitrarily connecting an "exponential tail" on the function at the arbitrary point, $\psi = 0.16$. This has little effect on the heat transfer since ψ is small over this portion of the range of large B values. An asymptote of 0.06 has been chosen for ψ (as suggested in ref. 1). The ψ function is illustrated in sketch (d). The slope of the linear portion of the ψ curve, C_ψ, depends on the read-in constant, A_5, as well as on M_p. Values in the neighborhood of 1.7 have been used for A_5 (ref. 7); however, the slope is preferably evaluated by wind-tunnel experiment. The C_ψ dependence on M_p is taken as a negative one-third power (ref. 7) in equation (77a). The other constants used depend on C_ψ. We use:

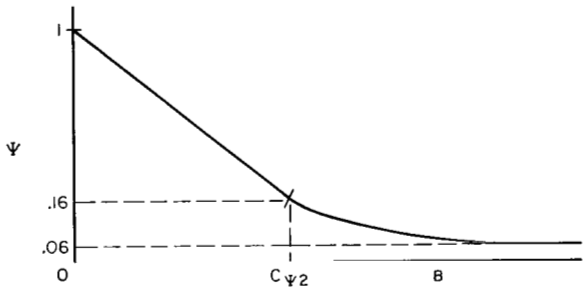

Sketch (d).- Blowing factor.

$$C_\psi = \frac{A_5}{M_p^{1/3}} \tag{77a}$$

$$C_{\psi_2} = \frac{0.84}{C_\psi} \tag{77b}$$

$$C_{\psi_3} = 10C_\psi \tag{77c}$$

For the ψ function we use:

$$\psi = 1 - C_\psi B \qquad \text{for} \quad B \le C_{\psi_2} \tag{78a}$$

$$\psi = 0.1e^{8.4-C_{\psi_3}B} + 0.06 \qquad \text{for} \quad B > C_{\psi_2} \tag{78b}$$

Radiation Energy Rate

With the arbitrary heating-rate programs, the incoming radiation as a function of time is a programmed input. For the calculated heating-rate programs, the gas cap radiation into the body is evaluated with an empirical approximation as in reference 1 (see also ref. 8)

$$q_R = E_4 R D^{E_5} V^{E_6} \overline{K}_{tu} \tag{79}$$

where the level of radiation and the surface reflectivity are included in E_4. Typical values of the constants used for earth entries are: $E_4 = 0.76\times10^{-6}$; $E_5 = 0.5$; $E_6 = 7.0$.

For both types of computing programs, the net radiation into the body is the difference between q_R and the reradiation out.

$$q_{rad} = q_R - \sigma\varepsilon T_w^4 \tag{80}$$

For charred surfaces, values of ε from 0.75 to 1.0 have been used.

Homogeneous Combustion Energy Input Rate

The model that we use for homogeneous combustion contains the assumption that this oxidation occurs at a flame front located at the outer edge of the boundary layer. The energy released by the reaction increases the enthalpy potential and this, in turn, increases the convective heat transfer to the surface. Thus, only a fraction of the energy released actually goes into the body. In the calculation, we make use of the mass rate of air flow per unit area into the boundary layer, $\dot{m}_{air} = (\rho_{air} v_{air})_e$, as calculated in equation (25). We also use the rate of expulsion of pyrolysis gases, $\dot{m}_{gw} = \dot{m}_g(0, t)$, as evaluated in equation (20b) or (21c) for $y = 0$.

The energy liberated by combustion of a unit mass of pyrolysis gas, h_{gc}, can be described as a function of temperature and extent of oxidation which will depend on a number of factors (evaluated in the material properties subprogram), or it can be conveniently approximated as a read-in constant. (The latter is within the framework of the simple flame front model assumed.) A value of about 11,000 cal/g has been used for h_{gc}. If there is a deficiency of oxygen, the value of h_{gc} must be corrected to an effective value, h_{gce}, which is the actual energy released per unit mass of pyrolysis gas. We have

$$h_{gce} = h_{gc} \qquad \text{when} \quad \dot{m}_{\substack{ox \\ ex}} > 0 \tag{81a}$$

$$h_{gce} = h_{gc}\left(\frac{\dot{m}_{ox}}{\dot{m}_{\substack{ox \\ theo}}}\right) \qquad \text{when} \quad \dot{m}_{\substack{ox \\ ex}} = 0 \tag{81b}$$

where $\dot{m}_{ox}$ and $\dot{m}_{\substack{ox \\ theo}}$ are evaluated in equations (26) and (27), respectively, and $\dot{m}_{\substack{ox \\ ex}}$ is evaluated from equations (28) and (29b). The rate of energy liberation at the flame front is

$$\dot{E}_{ff} = \dot{m}_{gw} h_{gce} \tag{82}$$

The increase of enthalpy potential at the edge of the boundary layer is the increment of energy, $\dot{E}_{ff}$, per unit mass of external gas entering the boundary layer. In $km^2 sec^{-2}$, we have

$$\Delta_{V^2} = \frac{0.00836\dot{E}_{ff}}{\dot{m}_{air}} \tag{83}$$

where $\dot{m}_{air}$ is evaluated in equation (25). The heat received by the body from the homogeneous combustion is in proportion to the increment in enthalpy potential, and this is:

$$q_{cg} = \frac{q_w \Delta_{V^2}}{V^2 - 0.00836 \overline{c}_p T_w} \tag{84}$$

Heterogeneous Combustion and Erosion Energy Rates

We assume that all energy liberated by heterogeneous (solid) combustion and erosion (material removal by other than combustion or sublimation) is received by the body since these are surface reactions. We include both energies in a solid combustion term.

$$q_{cs} = \dot{m}_{chcomb} h_{scomb} + \dot{m}_{chero} h_{sero} \tag{85}$$

The energies, h_{scomb} and h_{sero}, can be made functions of temperature (in the material properties subprogram); or they can be assigned constant values. The combustion energy, h_{scomb}, is per unit mass of char consumed, and the fraction of noncombustible material in the char must be considered in selecting h_{scomb} (see eq. (43)). (If the noncombustible material melts off with a heat of fusion, h_{scomb} should be modified to account for this energy.) Values of h_{scomb} between 1200 and 2500 cal/g have been used. The erosion energy, h_{sero}, is normally assigned the value, zero.

Sublimation Energy Rate

The sublimation of char is treated as a surface reaction which removes heat from the body. The heat of sublimation of the char, h_{sub}, can be set up as a function of temperature, but it is most conveniently read in as a constant positive number. It is an energy per unit mass of char consumed and will therefore depend on the composition of the char. One will normally use a heat of sublimation for carbon reduced by dividing by C_{kdb} to account for the fraction of carbon in the char. If the other material in the char is considered to melt with a heat of fusion when the carbon sublimes, a correction for this should be included in h_{sub}. A value of h_{sub} = 2700 cal/g has been used for some chars. The energy term due to sublimation turns out to be very small unless the flight velocity is extremely large, as from a planetary return. Thus

$$q_{sub} = -\dot{m}_{chsub} h_{sub} \tag{86}$$

where q_{sub} is positive for energy put into the body.

Boundary Conditions

A boundary condition for equation (1) is needed at the front surface of the body (y = 0). For the semi-infinite formulation, this is the only boundary condition. For the finite depth formulation, a back surface boundary condition is also required.

The front-face boundary condition is obtained from a surface energy balance.

$$q_w + q_{cg} + q_{cs} + q_{sub} + q_{rad} = -\overline{\overline{K}}_{sw} \left(\frac{\partial T}{\partial y}\right)_w \tag{87a}$$

Equation (87a) describes a relationship between $(\partial T/\partial y)_w$ and the energy rate terms on the left side of the equation. The evaluations used for the energy terms are listed in preceding sections. The values of the various energy terms depend on external flow conditions and on surface temperature; some of the evaluations depend on conditions in the interior of the body (including past history). The stability of equation (87a) is discussed in the section, Some Features of the Computer Program.

In the finite depth formulation, the heat shield is supported by a backing material (which may be a composite). The back surface energy balance for the heat-shield material is:

$$q_{BF} = \overline{\overline{K}}_{sBF} \left(\frac{\partial T}{\partial y}\right)_{BF} \tag{87b}$$

where $q_{BF} > 0$ means that heat is transferred into the heat shield. For the backing material, we also have an equation similar to (87b). The two surface temperature gradients depend on the back-face temperature and on internal temperatures in the heat shield and the backing material, and therefore they depend on the time history of the problem up to time, t. Complicated cases can require iteration to obtain "nearly exact" solutions for the back-face temperature. In actual numerical calculations, iteration is almost never required for good approximations. One simple method is to use $\overline{\overline{K}}_{sBF}$ from the previous (known) time line. A polynomial passed through the last several points of the current (being calculated) time line gives a linear relation between q_{BF} and T_{BF}. The same procedure can be used for the front of the backing material if it is solved by finite differences. Thus, two relations between q_{BF} and T_{BF} provide a solution.

The back-face temperature, T_{BF}, and the gradient in the heat shield, $(\partial T/\partial y)_{BF}$, are solved for in a back surface subprogram, QBACK. One particularly simple case (programmed in a QBACK) considers the backing material as a heat sink of finite heat capacity at a uniform, time-varying temperature, T_{BF}. For this case

$$q_{BF} = -\overline{c} \left(\frac{\partial T}{\partial t}\right)_{BF} \tag{87c}$$

where $\overline{c}$ is the heat capacity per unit area of the backing material. This case is also solved by using a polynomial to relate the unknowns, q_{BF} and T_{BF}, in equation (87b). The second relationship, in equation (87c), is obtained by approximating $(\partial T/\partial t)_{BF}$ as a finite forward difference quotient using the unknown, T_{BF}. The adiabatic case is obtained with $\overline{c} = 0$.

Trajectory Equations

For flight cases with aerodynamically calculated heating rates we need trajectory equations which are solved simultaneously with the other calculations. Trajectory equations are not used for flight cases with arbitrary heating rates (programmed as inputs).

The trajectory equations are in a trajectory subprogram. We use two-dimensional trajectory equations for entry in a meridional plane and allow the body mass to vary. Equations (88) through (95) are identical in form with equations (52) through (59) in reference 1. (See also ref. 9.)

$$V_\infty = \sqrt{u^2 + v^2} \tag{88a}$$

$$\gamma = \tan^{-1}\left(\frac{v}{u}\right) \tag{88b}$$

$$\frac{du}{dt} = \frac{-DV_\infty}{20\left(\frac{M}{C_D A}\right)}\left[u + \left(\frac{L}{Dr}\right)v\right] - \frac{uv}{R_{pl}} \tag{89a}$$

$$\frac{dv}{dt} = \frac{u^2}{R_{pl}} - \frac{g_{pl}}{10^5} - \frac{DV_\infty}{20\left(\frac{M}{C_D A}\right)}\left[v - \left(\frac{L}{D_r}\right)u\right] \tag{89b}$$

$$\frac{dD}{dt} = -\frac{Dv}{S_h} \tag{90}$$

We use a hypersonic approximation that considers the ambient enthalpy as a constant.

$$V = \sqrt{V_\infty^2 + E_{12}} \tag{91a}$$

$$E_{12} = 0.00836h_\infty \tag{91b}$$

where h_∞ is the average ambient enthalpy in cal/g and E_{12} has the units km^2sec^{-2}. For earth entries, 0.5 has been used for E_{12}.

For earth entries, we generally use an option in the computing program that puts in the ARDC atmosphere. This is actually approximated as an exponential atmosphere with three successive values of the scale height, S_h, which automatically change with altitude as programmed. The option also sets $R_{pl} = 6440$ km and $g_{pl} = 980$ cm/sec^2. Another option, for arbitrary planet entries, accepts read-in values for R_{pl} and g_{pl}, arbitrary scale heights (initial, two intermediate, and a final value), and atmospheric densities at which the scale heights change.

The quantity, M/C_DA (g/cm^2), is needed in the trajectory equations. The variation of M/A has been related empirically to the surface recession, X, as in reference 1. This is equivalent to assuming a geometry for the recession shape.

$$\frac{M}{A} = \left(\frac{M}{A}\right)_i \left[1 + E_{18}X + C_3\left(e^{C_4X} - 1\right)\right] \tag{92}$$

The variation of the drag coefficient, C_D, through the free-molecule, transitional, and continuum regimes is represented by

$$C_D = C_{DC}\left[1 + E_9\, e^{-15(RD)(1+E_{13})}\right] \tag{93}$$

where

$$E_9 = \frac{C_{DFM} - C_{DC}}{C_{DC}} \tag{94}$$

and E_9 depends on body shape. The free-molecule drag coefficient, C_{DFM}, may be given the value, 2. The parameter, E_{13}, has some dependence on body shape (and flight conditions), but will often be assigned the value zero, which is the value for a sphere in air. Combining equations (92) and (93) yields

$$\frac{M}{C_DA} = \left(\frac{M}{C_{DC}A}\right)_i \frac{\left[1 + E_{18}X + C_3\left(e^{C_4X} - 1\right)\right]}{\left[1 + E_9\, e^{-15(RD)(1+E_{13})}\right]} \tag{95}$$

In equation (95), C_{DC} is grouped with the initial value of $M/C_{DC}A$; this initial grouped quantity is read into the computing program. The empiricism in equation (95) can also be used to account for any change in C_{DC} with change of body shape.

Calculated Quantities of Interest

The two quantities listed below are calculated by the computing program because they are considered to be of interest. They are not needed in any other calculations. They are also listed in reference 1.

Thermal thickness-We define thermal thickness as

$$\Delta = - \frac{(T_w - T_o)}{(\partial T/\partial y)_w} \tag{96}$$

This quantity is meaningful only when the wall temperature gradient is negative.

Stored energy comparison with exponential temperature profile-We compare each temperature profile with an exponential profile having the same $(\partial T/\partial y)_w$. We define the quantity, ϕ, as the ratio of energy stored to the energy stored by the corresponding exponential profile (with form similar to equation (122)). Both energies are calculated as constant property approximations.

$$\phi = \frac{\int_o^{y_{BF}} (T - T_o) dy_1}{\Delta (T_w - T_o)} \tag{97}$$

This quantity, ϕ, is only meaningful when $\Delta > 0$, or the wall temperature gradient, $(\partial T/\partial y)_w$, is negative.

Energy Balance

As an indication of the accuracy of solutions obtained by the numerical finite difference method used, an energy rate balance is made from the solution at hand. The group of energy rate terms listed below are evaluated and summed up; the residual of the sum is the error in the energy rate balance. The magnitudes of the energy rates are also of interest since these show the dispositions of the various energies.

The sum of the energy rate terms includes q_w, q_{rad}, q_{cg}, q_{cs}, and q_{sub}. These are evaluated in equations (66), (70), or (73d) for q_w, (80), (84), (85), and (86), respectively. These are the terms on the left side of the front-face boundary condition equation (87a). The energy rate into the back surface, q_{BF}, is given in equation (87b). This term is zero for the semi-infinite formulation.

We require an evaluation of the stored energy in the material. For the enthalpy of the solid material (cal/g), we have, from equation (13b):

$$h_s = \int_o^T c_s \, dT_1 = \int_o^T [(1 - J)c_{ch} + Jc_p]dT_1 \tag{98}$$

For the enthalpy of the gas (cal/g), we write

$$h_g = \int_o^T c_{pg} \, dT_1 - h_{sref} \tag{99}$$

where $-h_{sref}$ is the energy of formation of the gas at 0°K. (For a pyrolysis reaction that is endothermic at 0°K, $h_{sref} < 0$.) The enthalpy per unit area per unit depth is then

$$\bar{h}(y, t) = \rho_s h_s + \rho_g h_g \tag{100}$$

where ρ_s and ρ_g are evaluated in equations (11) and (18), respectively. The stored energy is then

$$\bar{h}_T(t) = \int_o^{y_{BF}} \bar{h}(y_1, t)dy_1 \tag{101}$$

For the rate of increase of stored energy,

$$q_{stor} = \frac{d\bar{h}_T}{dt} = \frac{d}{dt} \int_o^{y_{BF}} \bar{h}(y_1, t)dy_1 \tag{102}$$

This is evaluated by the computer program as a finite difference quotient, the numerator being the difference between values of $\bar{h}_T$ for adjacent time lines and the denominator being Δt. With the finite depth formulation, y_{BF} shrinks with time. With the semi-infinite formulation, y_{BF} remains constant, but actually an infinite depth is being represented by a finite one. This finite depth must be sufficiently deep that what is cut off is of no consequence. This requires that, to within a desired degree of accuracy:

$$T_{BF} = T_o$$

$$\left(\frac{\partial T}{\partial y}\right)_{BF} = 0$$

$$J_{BF} = 1$$

$$\rho_s(y_{BF}, t) = \rho_p$$

$$\dot{m}_g(y_{BF}, t) = 0$$

These requirements also must hold in the immediate vicinity of the (fictitious) back face. The above requirements do not hold for the finite depth case.

The convection energy rate of solid and gaseous ablative material (positive out), for the semi-infinite formulation, is:

$$q_{vcon} = \overline{v}_s[\rho_s(y_{BF}, t)h_s(y_{BF}, t) - \rho_s(0, t)h_s(0, t)] + \dot{m}_g(0, t)h_g(0, t) \tag{103a}$$

The depth requirements noted above for a semi-infinite representation insure that q_{vcon} is correctly evaluated for this case.

With the finite depth formulation, the control volume is shrinking and no material is entering it; thus:

$$q_{vcon} = -\overline{v}_s\rho_s(0, t)h_s(0, t) + \dot{m}_g(0, t)h_g(0, t) \tag{103b}$$

The energy rate balance is:

$$q_{res} = q_w + q_{rad} + q_{cg} + q_{cs} + q_{sub} + q_{BF} - q_{vcon} - q_{stor} \tag{104}$$

where $q_{BF} = 0$ for the semi-infinite formulation and where q_{res} is the residual term in the energy rate balance. We define (arbitrarily) the error in the energy rate balance as

$$e = \frac{q_{res}}{|q_w|} \quad \text{when} \quad |q_w| > 1 \tag{105a}$$

$$e = q_{res} \quad \text{when} \quad |q_w| \leq 1 \tag{105b}$$

We also calculate a cumulative energy balance. This balance shows the total size of the various energy terms and the error accumulation. We compute the integrals:

$$Q_w = \int_{t_i}^{t} q_w \, dt_1 \tag{106a}$$

$$Q_{rad} = \int_{t_i}^{t} q_{rad} \, dt_1 \tag{106b}$$

$$Q_{cg} = \int_{t_i}^{t} q_{cg} \, dt_1 \tag{106c}$$

$$Q_{cs} = \int_{t_i}^{t} q_{cs}\, dt_1 \tag{106d}$$

$$Q_{sub} = \int_{t_i}^{t} q_{sub}\, dt_1 \tag{106e}$$

$$Q_{BF} = \int_{t_i}^{t} q_{BF}\, dt_1 \tag{106f}$$

(where $Q_{BF} = 0$ for the semi-infinite formulation).

$$Q_{vcon} = \int_{t_i}^{t} q_{vcon}\, dt_1 \tag{106g}$$

$$Q_{stor} = \overline{h}_T(t) - \overline{h}_T(t_i) \tag{106h}$$

The accumulated residual is

$$Q_{res} = Q_w + Q_{rad} + Q_{cg} + Q_{cs} + Q_{sub} + Q_{BF} - Q_{vcon} - Q_{stor} \tag{107}$$

Representations of Physical Properties

In the analysis, the quantities, ρ_p and ρ_{ch}, the densities of virgin plastic and pure char, respectively, are taken as constant. Other properties of the virgin plastic and pure char, such as specific heat, enthalpy, and thermal conductivity are generally functions of temperature. The temperature variation applies also to the specific heat and enthalpy of the pyrolysis gas. The temperature-dependent properties are evaluated for each given material in a material properties subprogram for the material. The properties data, which are in the subprogram, may be in tabular or equation form.

Some physical properties can be described for a number of materials by more or less universally accepted equation forms (e.g., kinetic reaction rates), as given in the analysis above; the constants in the equations are "read-in" quantities. These equations are "built into" the analysis, but more complex representations can generally be obtained by prescribing a variation of the constants through the use of the material properties subprogram.

For a given material, the physical properties of the virgin plastic and the pure char are generally determined by standard measurement techniques. The thermal conductivity of the pure char is probably the most uncertain quantity. (Some measurements even indicate a hysteresis effect for this quantity; see ref. 10.) For a given material, comparisons should be made between ablation calculations and wind-tunnel measurements, because the "effective" values (in the wind tunnel) of the physical properties, particularly $\overline{\overline{K}}_{ch}$, may be

somewhat different from those values determined from direct property measurements. When this occurs, the $\bar{\bar{K}}_{ch}$ is usually adjusted to obtain good wind-tunnel comparisons, and the adjusted values are also used for flight calculations. In the material properties subprograms, adjusted values of properties are usually put in. However, the adjustment can often be made by applying a constant multiplier to the measured values. Then, one would enter measured values and use an available (open) read-in constant as a multiplier.

NUMERICAL ANALYSIS AND COMPUTATION PROCEDURES

In the above analysis, the energy equation (1) with its boundary conditions, equation (87), is the principal equation system to be solved. Most of the other equations listed are used to evaluate quantities that appear in equation (1) and its boundary conditions, equation (87). Cases of interest are not generally amenable to analytical solutions, so numerical methods must be used. Equation (1), a parabolic partial differential equation, is solved numerically by finite differences using an explicit (forward difference) scheme. As the solution advances from one time line to the next, the first quantity solved for is the finite-differenced temperature array, T(M), from which the various temperature-dependent physical properties are determined. Also, the quantities, K(M), then z(M), leading to J(M) and ρ_s(M), are calculated by means of the temperature array. At this point, we also calculate the rate of generation and flow of pyrolysis gases, $\dot{w}_g$(M) and $\dot{m}_g$(M), and the surface recession rate, $\dot{X}$. These quantities become new inputs to equation (1) in advancing to the next time line.

Finite Differencing

In the finite differencing scheme used to solve equation (1), the partial derivatives of the temperature, T, are represented by the following difference quotients:

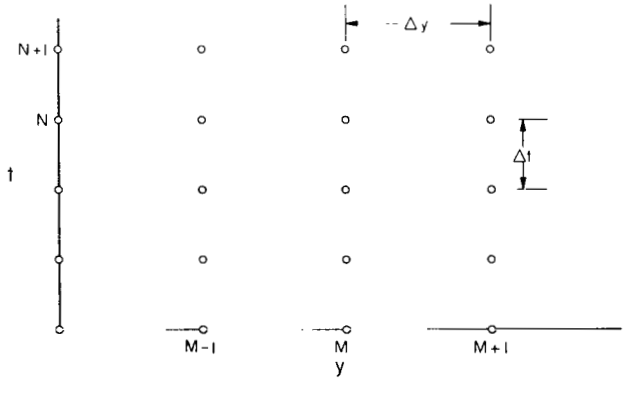

Sketch (e).- Finite differencing scale.

$$\left(\frac{\partial T}{\partial t}\right)_{M,N} = \frac{T_{M,N+1} - T_{M,N}}{\Delta t} \tag{108}$$

$$\left(\frac{\partial T}{\partial y}\right)_{M,N} = \frac{T_{M+1,N} - T_{M-1,N}}{2\Delta y} \tag{109}$$

$$\left(\frac{\partial^2 T}{\partial y^2}\right)_{M,N} = \frac{T_{M+1,N} - 2T_{M,N} + T_{M-1,N}}{(\Delta y)^2} \tag{110}$$

where M-1, M, M+1 are grid point numbers on the depth (y) scale, and N, N+1 are numbers on the time (t) scale as shown in sketch (e). Finite increments are indicated by the Δ symbol.

Stability and Accuracy of the Finite Difference Equation

In solving a parabolic partial differential equation by forward differences, a stability requirement is necessary so that round-off and other errors do not grow excessively large. The forward finite difference form of equation (1) has an approximate stability parameter requirement

$$Z_x = \frac{\Delta t \bar{\bar{K}}_s}{(\Delta y)^2 [\rho_s c_s + \rho_g c_{pg}]} \leq \frac{1}{2} \tag{111}$$

that may not be sufficient to guarantee stability of the entire calculation. If an instability develops (say, at the front face, or at the back face for finite depth calculations), as a general rule one can arbitrarily reduce Z_x until stability is obtained. This is discussed further in the next section. The stability parameter, Z_x, is printed out for each finite-differenced grid point at each time printed so that the stability of the calculations can be monitored continuously. Usually Z_x will be largest with the smallest Δy used in finite differencing. This is Δy_2, which is shown in sketch (h) in appendix C.

A gross check on the accuracy of numerical solutions is provided by the running energy balance and the cumulative energy balance described above. An additional check, standard in numerical work, can be made by adjusting the time and space increments, Δt and Δy, and noting the effect on the numerical solutions. This check determines the adequacy of representing the partial derivatives by difference quotients with the finite increments as selected.

Some Features of the Computer Program

Damping-Within the requirement of the stability parameter, $Z_x \leq 1/2$, the overall calculation may still not be stable mainly because Arrhenius type functions of temperature are used that are quite volatile at temperatures above a threshold value. In general, the calculations become more stable when smaller Z_x values are used. This can be accomplished by making Δt smaller or Δy larger. However, if Δy is made too large, the space derivatives are poorly represented by the difference quotients used, particularly at the front face where the space derivative may be quite large. A value of Δy too large may then give an excessively high surface temperature or require an excessively low temperature at the adjacent finite-differenced grid point. Thus, too large a value of Δy can render the front-face boundary condition (eq. (87a)) unstable. Reducing the Δt increment to very small values will improve stability but will increase computing machine time, which varies inversely as Δt.

To avoid excessively small time increments, an option is provided in the computing program that allows damping of the calculated changes in certain quantities. These are calculated quantities that tend to "overshoot" or oscillate, and damping serves to suppress the oscillation. The damping formula

used is:

$$X_c = X_{-1} + d(X_p - X_{-1}) \tag{112}$$

where X is the quantity considered (modified by subscripts); X_{-1} represents the corrected value of X from the previous time line, X_p is the predicted value of X for the current time line as obtained from the equations given in the analysis, and X_c is the corrected value of the quantity, X. The symbol, d, represents the damping constant where $0 < d \leq 1$. It is seen that $d < 1$ proportionately reduces the change in the quantity, X, from one time line to the next. When $d = 1$, the predicted and corrected values of X are identical, and there is no damping. When damping is used, it overrides or modifies the normal computations. Damping is available in the computing program to correct any or all of the following quantities separately: T_w, $\dot{m}_g(y, t)$, $\dot{m}_{chcomb}$, $\dot{m}_{chero}$, $\dot{m}_{chsub}$, ψ. The corrected values are calculated as the step immediately after predicted values are determined so that subsequent calculations (and determinations of other quantities) use the corrected values. Separate damping constants are read into the computing program for each of the quantities listed; each damping constant can be changed twice during a run. The latter provision allows a discrete application of damping when it is needed, as for example, during rapid changes in external conditions acting on an ablator.

The application of damping should be minimized ($d \to 1$) to that amount necessary to smooth or reduce oscillations. Excessive damping can delay the variation of a calculated quantity in its approach to the correct calculated value. The use of damping requires some judgment, and may involve some trial and error and repeated calculations. In this connection, important criteria are the residual rate, q_{res}, and the accumulated residual, Q_{res}, in the energy balances. The residuals should, obviously, be minimized. In damping the T_w calculation, another important criterion is the change in $(\partial T/\partial y)_w$; the method of using this criterion is explained below.

Front-face boundary condition-The front-face boundary condition equation (87a) furnishes a nonlinear relationship between T_w and $(\partial T/\partial y)_w$, but also involved in this equation are the internal temperature distribution and the extent of degradation of the material. The terms q_w, q_{cg}, and q_{cs} are affected by the rate of expulsion of pyrolysis gases, and the rate of gas expulsion depends on the interior temperature distribution and the extent of degradation. The extent of degradation at a time, t, obviously depends on the entire past history of the problem. The energy rate terms on the left side of equation (87a) also depend on external conditions which may be changing with time (as for example, with an entry flight). We see that, in order to solve equation (87a) for the boundary conditions at time, t, we must have solved the entire problem up to time t.

Using a forward difference scheme to solve the partial differential equation (1), we obtain the internal temperatures for the next time line. For the front surface temperature, we seek a numerical solution to equation (87a). We could iterate a solution to equation (87a) by requiring that T_w and $(\partial T/\partial y)_w$ fit a polynomial that passes through several interior grid points. This

consumes computing time, because terms on the left side of equation (87a) depend on T_w, and would have to be recalculated with every iteration cycle.

In place of iteration, we use (with little loss of accuracy) the following scheme in the computing program. We set up a two-term Taylor series:

$$\left(\frac{\partial T}{\partial y}\right)_{wc'} = \left(\frac{\partial T}{\partial y}\right)_{we_{-1}} + \left[\frac{d}{dT_w}\left(\frac{\partial T}{\partial y}\right)_{we_{-1}}\right]\left(T_{wp} - T_{w_{-1}}\right) \tag{113}$$

where the subscript -1 means from the previous time line, and

$$\frac{d}{dT_w}\left(\frac{\partial T}{\partial y}\right)_{we_{-1}} = -\left\{\frac{1}{\bar{\bar{K}}_{sw}}\frac{d}{dT_w}\left[q_w + q_{cg} + q'_{cs} + q_{sub} + q_{rad}\right]\right\}_{-1}$$

$$-\left\{\left(\frac{\partial T}{\partial y}\right)_{we}\frac{1}{\bar{\bar{K}}_{sw}}\cdot\left(\frac{d\bar{\bar{K}}_{sw}}{dT_w}\right)\right\}_{-1} \tag{114}$$

Equation (114) contains $(d/dT_w)q'_{cs}$. The term q_{cs} as evaluated in equation (85), includes the heat liberated by erosion (if $h_{sero} \neq 0$). For equation (114), q_{cs} is modified and q'_{cs} is defined as:

$$q'_{cs} = \dot{m}_{chcomb} h_{scomb} \tag{115}$$

thus the erosion term is neglected in calculating the predicted surface temperature, T_{wp}. This is exact in the usual case when $h_{sero} = 0$. Otherwise, it is approximate, but an erosion term in equation (114) should always be small. To include this term would involve several equation forms to correspond to the different empirical forms for evaluating erosion itself (eq. (46)). Equation (113) has the form:

$$\left(\frac{\partial T}{\partial y}\right)_{wc'} = A + B(T_{wp} - T_{w_{-1}}) \tag{116}$$

We also evaluate $(\partial T/\partial y)_{wc'}$ by means of a cubic passed through the first four (finite difference) calculated grid points of T. (See sketch (h), appendix C.)

$$\left(\frac{\partial T}{\partial y}\right)_{wc'} = \frac{1}{\Delta y_2}\left[-\frac{11}{6}T_{wp} + 3T_{L2} - \frac{3}{2}T_{L3} + \frac{1}{3}T_{L4}\right] \tag{117}$$

The increment, Δy_2, is the forwardmost Δy used in the finite difference equation, as indicated in sketch (h). Equation (117) has the form:

$$\left(\frac{\partial T}{\partial y}\right)_{wc'} = -\frac{11}{6\Delta y_2} T_{wp} + C \tag{118}$$

Combined equations (116) and (118) become:

$$T_{wp} = \frac{C - A + BT_{w-1}}{B + (11/6\Delta y_2)} \tag{119}$$

The computer prints T_{wp} as a quantity of interest. It is inserted into equation (112) to obtain the corrected surface temperature, T_{wc}, which is the value used (and also printed out). We obtain a corrected calculated value of the front surface temperature derivative by rewriting equation (117).

$$\left(\frac{\partial T}{\partial y}\right)_{wc} = \frac{1}{\Delta y_2}\left[-\frac{11}{6} T_{wc} + 3T_{L2} - \frac{3}{2} T_{L3} + \frac{1}{3} T_{L4}\right] \tag{120}$$

Once a corrected value of surface temperature, T_{wc}, is determined for the new time line, the terms on the left side of equation (87a) can be evaluated. Then, from equation (87a), the surface temperature gradient, now labeled $(\partial T/\partial y)_{we}$, that satisfies the surface energy balance can be evaluated. If the calculations would be perfect, we would have

$$\left(\frac{\partial T}{\partial y}\right)_{wc} = \left(\frac{\partial T}{\partial y}\right)_{we} \tag{121}$$

or the two methods of calculation should yield the same answer. (Iteration would accomplish this to a desired degree of accuracy.) For comparison, the computer prints both evaluations of $(\partial T/\partial y)_w$. The closeness of the comparison furnishes a criterion for possible adjustment of the time and distance spacing and, if necessary, damping in the T_w calculation.

The evaluation $(\partial T/\partial y)_{we}$ is used as $(\partial T/\partial y)_{we_{-1}}$ in equation (113) in making the calculations for the next time line. With the procedure used, a small oscillation is expected in the value of T_w about the true value, but the oscillation is self-correcting. For example, if T_w is too high, the energy rate terms on the left side of equation (87a) will be too small, and the absolute value of $(\partial T/\partial y)_{we}$ calculated from equation (87a) will also be too small. This will reduce the value of T_w as calculated for the next time line, so that corrective action will occur from one time line to the next.

Back boundary condition-In the semi-infinite formulation of the problem, there is no back boundary condition. In the numerical solution of

equation (1), however, we are actually representing an infinite depth with a finite depth having a finite number of grid points. The deepest point is assigned the temperature, T_o, which it holds for all time. An initial temperature profile must be selected such that the grid point adjacent to the deepest point has the temperature T_o to within a desired accuracy. Also there should be no degradation at either of these points (J = 1). The point adjacent to the deepest point is watched during a calculated run. It should experience essentially no degradation (J = 1) and the temperature should remain at T_o to within some desired accuracy. If these criteria are not met, more depth is needed (to represent infinity).

In the finite depth problem, we have the back boundary condition, equation (87b). This is solved in a back surface subprogram for T_{BF} and $(\partial T/\partial y)_{BF}$, and q_{BF} is also obtained (in the main program) from equation (87b). For the simple finite heat sink type of backing, the calculation also makes use of equation (87c).

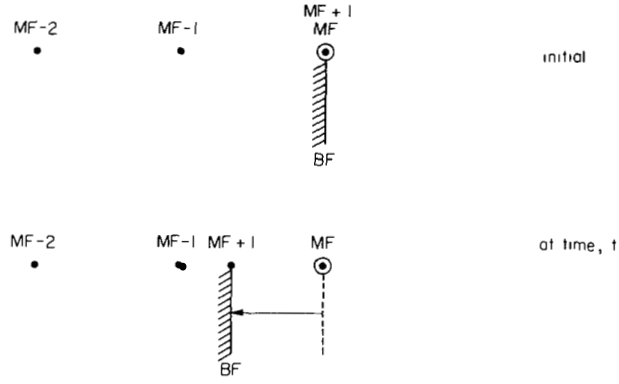

Sketch (f).- Back-face grid spacing.

As the front surface recedes with time, the material depth decreases. Since the origin of the coordinate system is kept at the front face, the spacing between the back-face grid point and the adjacent point is allowed to decrease. (The printout shows the depth back of the front face of each grid point.) As indicated in sketch (f), the initial array consists of MF grid points with an MF+1 point that coincides with the MF point at the back face. As the back face of the material moves forward, the MF+1 point moves with it. The MF point remains fixed in space, and thus becomes a virtual point. The temperature of the virtual point, T_{MF}, is calculated as a linear extension of the profile in the material. This temperature is used in calculating the next time line (because of the convenience of using the uniform spacing of the virtual point). It is printed out as a quantity of interest, not as part of the regular array of y, T, J, etc., at the grid points. When the surface recession, χ, exceeds the spacing between grid points at the back (in the sketch the back face, BF, moves ahead of grid point, MF-1), one node is dropped at the back. Thus, the numerical values of all the grid points shown in the sketch are reduced by one, and the calculation procedure is the same as before.

At the back face, it is possible for instability to develop when the stability parameter, $Z_\chi \leq 0.5$. If this occurs, Z_χ should be made arbitrarily smaller until stability is obtained.

Starting Values

To start the solution to equation (1) (which is parabolic), it is necessary to assign initial conditions. The particular selection of initial conditions is generally not critical as their influence damps out in a short time. The equations developed in this section are similar to those developed in appendix B of reference 1.

Continuation type program-With a continuation type computing program, none of the equations shown below in this section are used. The initial temperature profile is read into the program (also the profiles of extent of degradation and rate of gas expulsion). These arbitrarily read-in profiles are generally the final profiles of a calculation that was interrupted and is now being continued.

Starting type programs-With starting type computing programs, we assume we have virgin plastic material (J = 1 everywhere). The temperatures should be sufficiently low that they could exist before the onset of ablation. The initial temperature profile that we assume is exponential.

$$T_i(y) = T_o + (T_{wi} - T_o)e^{-\frac{y}{\Delta_i}} \tag{122}$$

If T_{wi} is selected near T_o, this profile is a small perturbation on a constant T_o profile. We take the y derivative of T_i at $y = 0$, equate it to the ratio of the heat flux (eq. (87a)) to thermal conductivity, and solve for the initial thermal thickness, Δ_i. (See eq. (96).)

$$\Delta_i = \frac{\bar{\bar{K}}_{pwi}(T_{wi} - T_o)}{q_{wri}} \tag{123}$$

where

$$q_{wri} = q_{wi} + q_{radi} \tag{124}$$

is the combined initial convective and radiative heat flux.

Arbitrary heating-rate programs (starting type)-Equations (124), (123), and (122) are used in that order to obtain the starting profile. The quantities, q_{wi} and q_{radi}, in equation (124) are obtained from programmed inputs. The initial convection rate, q_{wi}, is the same as q_o obtained from an inversion of equation (72), where q_{ocw} is a programmed input and V^2 (eq. (56a)) is obtained from h_{st}, which is also a programmed input. For the initial net radiation input, q_{radi}, re-radiation is neglected (eq. (80)), and q_{radi} is equated to q_R, which is a programmed input.

Calculated heating-rate programs (starting type)-Equations (124), (123), and (122) are used in that order for the starting profile. However, as described under Flight Cases, one option allows Δ_i to be assigned a value, instead of obtaining it from equation (123). The initial convective and radiative heat fluxes needed in equation (124) are obtained differently for

wind-tunnel and flight cases, as described later. Calculating q_{wi} and q_{radi} requires the initial free-stream density, D_i. For wind-tunnel calculations, D_i will be known; for flight, D_i can be assigned or calculated as will be described.

Ablation in a wind tunnel-The starting of a wind tunnel is considered as a sudden step of a heat flux. We assume that $\psi = 1$, so

$$q_{wi} = q_{oci} \tag{125}$$

and

$$q_{wri} = q_{oci} + q_{radi} \tag{126}$$

We evaluate q_{oci} from equation (62) and q_{radi} from equations (79) and (80), assuming negligible re-radiation and using T_{wi} for T_w. If T_{wi} is small, q_{wri} is approximately constant for a short period of time (eq. (62)). We approximate this case as the classical conduction problem with constant heat flux and constant properties (refs. 1 and 11), and we calculate the time at which the front face arrives at the assumed temperature, T_{wi}.

$$t_i = \frac{(T_{wi} - T_o)^2 \pi \rho_p c_{pwi} \overline{\overline{K}}_{pwi}}{4 q_{wri}^2} \tag{127}$$

We can set $T_{wi} \geq T_o$; the greater value is not necessary, but it gives the computing program a smooth start.

Flight with arbitrary initial conditions-In starting flight calculations, we can use an assigned initial velocity, V_{∞_i}, and a flight-path angle, γ_i, at (arbitrary) time, $t_i = 0$. Equivalent to a starting altitude, the initial atmospheric density, D_i, can be assigned as well as the initial thermal thickness, Δ_i. A value for T_{wi} is assumed and the initial temperature profile is obtained from equation (122). Using this procedure we do not require that Δ_i be consistent with the relationship in equation (123), but we still calculate q_{wi}, q_{radi}, and q_{wri}.

Initial conditions for entry flight-For entry flights an alternative starting procedure is described in appendix B of reference 1. An assigned V_{∞_i} and γ_i and an assumed T_{wi} are used to calculate the entry into an exponential atmosphere. Heating during this entry raises the front-face temperature from T_o to the assumed T_{wi}. The convective heating rate during this initial entry phase is considered to be a free-molecule type so we have:

$$q_{wi} = q_{FMi} \overline{K}_{tu} \tag{128}$$

and $\overline{K}_{tu}$ in equation (61) specializes to $\overline{K}$. Thus

$$q_{wi} = \overline{K} q_{FMi} \tag{129}$$

For the initial combined convective and radiative heating rate, equation (124) is written as

$$q_{wri} = \overline{K} q_{FMi} + q_{radi} \tag{130}$$

We evaluate q_{FMi} from equation (64) and q_{radi} from equations (79) and (80), and neglecting re-radiation, we have the heating rate at time, $t_i = 0$.

$$q_{wri} = \frac{\overline{K} A_{cq} D_i V_i}{0.0836} (V_i^2 - 0.00836 \overline{c}_p T_{wi}) + \overline{K} E_4 R_i D_i^{E_5} V_i^{E_6} \tag{131}$$

where we use V_i as an approximation for V_{∞_i}. In the assumed exponential atmosphere, we write the density as

$$D = c\, e^{-\left(\frac{Alt}{Sh_i}\right)} \tag{132}$$

where Alt represents altitude. During the entry phase from $t = -\infty$ to $t = t_i = 0$, the enthalpy potential can be approximated as constant, and the heating rate, q_{wr}, will increase exponentially as D increases. We can rewrite equation (131) for q_{wr} and substitute the variable D for D_i, and we can integrate the equation from $t = -\infty$ to $t = t_i = 0$ for the total heat absorbed.

$$Q_{total} = \frac{Sh_i \overline{K} A_{cq} D_i (V_i^2 - 0.00836 \overline{c}_p T_{wi})}{0.0836 \left|\sin \gamma_i\right|} + \frac{Sh_i \overline{K} E_4 R_i D_i^{E_5} V_i^{E_6 - 1}}{E_5 \left|\sin \gamma_i\right|} \tag{133}$$

The total heat absorbed is approximated as

$$Q_{total} \approx \rho_p c_{pwi} \int_o^{y_{MF}} (T - T_o) dy \tag{134}$$

and using the profile equation (122) we have approximately

$$Q_{total} \approx \rho_p c_{pwi} (T_{wi} - T_o) \Delta_i \tag{135}$$

We substitute q_{wri} from equation (131) into equation (123) for Δ_i, and put Δ_i into equation (135) to obtain:

$$Q_{total} \approx \frac{\rho_p c_{pwi} \overline{\overline{K}}_{pwi} (T_{wi} - T_o)^2}{\frac{\overline{K} A_{cq} D_i V_i}{0.0836} (V_i^2 - 0.00836 \overline{c}_p T_{wi}) + \overline{K} E_4 R_i D_i^{E_5} V_i^{E_6}} \tag{136}$$

We eliminate Q_{total} by combining equations (133) and (136) and we obtain an equation of the form

$$\left(D_i + \frac{K_a}{E_5} D_i^{E_5}\right)\left(D_i + K_a D_i^{E_5}\right) = K_b \tag{137}$$

where K_a and K_b are constants and D_i is the only unknown.

The procedure in starting an entry calculation is to assume a T_{wi}, and, knowing the scale height far out in the atmosphere, S_{h_i}, calculate D_i from equation (137). Next obtain q_{wri} from equation (131), and Δ_i from equation (123); then put Δ_i in the profile equation (122). The assumption of the T_{wi} determines the D_i, or equivalently, the altitude at which to start time zero. In order to have a finite starting altitude, it is necessary to select $T_{wi} > T_o$.

Use of Programs in Various Approximations

The analysis outlined above is for a blunt-body axisymmetric stagnation point. The approximate use of the analysis in the stagnation region of an arbitrary blunt body is considered quite valid. The analysis is actually one-dimensional, but in the stagnation region, lateral gradients of such quantities as temperature (and resulting heat transfer) are very small relative to gradients normal to the surface. The heat loading for any point for which calculations are being made must be known or calculated. The use of the analysis for points far fron the stagnation region is still more approximate, but it is often acceptable when these points have relatively small heat loadings, as is often the case.

In the analysis, the stagnation pressure, p_{t_2} or p_{s_2}, appears a number of times in the development. This should be considered to be the local external pressure, p_w, for off-stagnation calculations. This applies to equations (15), (24b), (37), (39), (40), (46a), (50), (51), and (52). For a flight case with calculated heat loadings, the constant, A_1, in equation (54) is adjusted to give the local external pressure p_w. For the calculations of local convective and radiative heat loadings, the constants to be adjusted are A_4, A_{cq}, A_5, and E_4 in equations (62), (64), (77a), and (79), respectively. In equation (62), if desired, the effective nose radius, R, may be changed along with A_4 by adjusting the constants in equation (60). For calculation of the oxygen available for combustion off the stagnation point, the constant $\overline{\phi}$ in equation (24b) may be assigned values other than unity. These same adjustments are also made for wind-tunnel cases with calculated loadings, except that the local pressure, p_w, is read in (FORTRAN symbol PT2). For off-stagnation calculations with arbitrary heating rates, the constants to be adjusted are $\overline{\phi}$, A_1, and A_5 in equations (24b), (54), and (77a), respectively. For these cases, equation (54) is inverted to yield the free-stream density, D, from the programmed p_{t_2} or p_w. The radius, R, is programmed as a function of time,

although R may be a fictitious effective quantity for many of these cases. The program calculates and uses (but does not print) A_4 from an inversion of equation (62).

The stagnation-point analysis developed implies the assumption of a laminar boundary layer with a laminar convective heat-transfer rate and diffusion rate. An off-stagnation point may have a turbulent boundary layer that will introduce a further approximation (and complication) in the analysis and computing programs. Equation (62) for q_{oc} is considered to be a laminar stagnation point form. A calculated turbulent q_{oc} rate may be obtained by adjustment of A_4 (and possibly R) in equation (62). This rate should be satisfactory for the constant conditions of a wind-tunnel calculation. For a flight case with calculated heating rates, the evaluation is more difficult. It may then be necessary to program A_4 (and possibly R) as functions of V and D in the atmosphere considered, to account for effects of time-varying Mach and Reynolds numbers for the point considered. (This could be done in the material properties subprogram.) For arbitrary heating-rate calculations the situation is somewhat better, as q_{ocw} is known and q_o can be obtained from equation (72). An effective R, as a function of time, can be programmed to be consistent with equation (62). For both the calculated and the arbitrary heating-rate types of calculations, A_5 in equation (77a) should be selected to give a realistic turbulent ψ function. The value of $\overline{\phi}$ in equation (24b) should probably also be adjusted (or programmed) for a turbulent boundary layer.

Illustrative Example

An example is given to illustrate a typical use of the numerical computing programs. This example is typical of Apollo flight conditions. The figures given show the time variation of some of the quantities of interest; a number of other quantities, not plotted, are also computed and printed out by the program. See appendix C for the read outs (for another case) from a typical printing subprogram.

This example calculation is for a body point in the stagnation region near but not at the stagnation point. This is then an approximation in the use of the program. (Experience has indicated that this approximation is quite good.) The trajectory and heat loadings in the example are assigned.

Figure 1 shows the assigned trajectory while figure 2 gives the total enthalpy, h_{st}, and surface pressure, p_w. The total enthalpy was calculated by combining equation (91a) with the inversion of equation (56). The surface pressure, p_w, was obtained by first calculating p_{t_2} using the hypersonic approximation, equation (54), with $A_1 = 1$. Then p_{t_2} was multiplied by a factor to obtain p_w. The multiplying factor p_w/p_{t_2} was obtained from the NASA Manned Spacecraft Center in a private communication. It had been determined from wind-tunnel tests of the model configuration at various angles of attack.

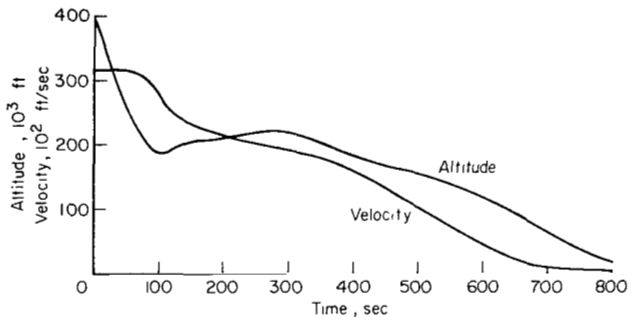

Figure 1.– Trajectory for illustrative example.

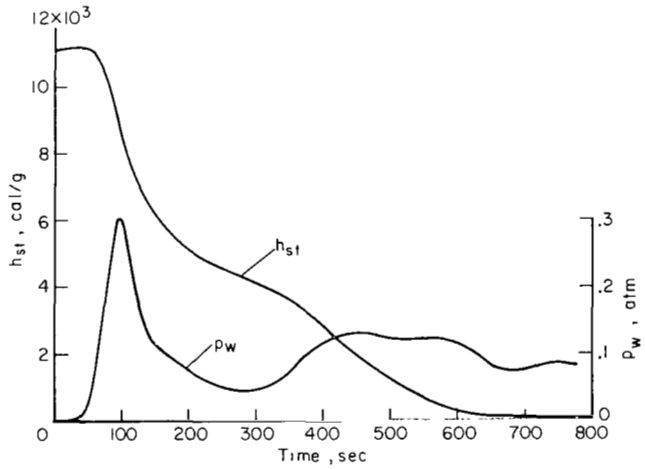

Figure 2.– Total enthalpy, h_{st}, and surface pressure, p_w, at a near-stagnation body point.

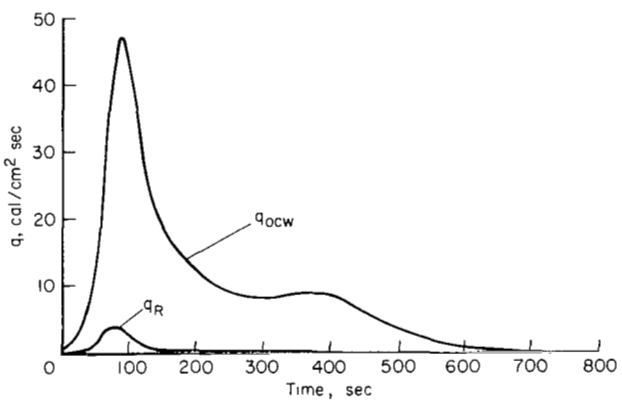

Figure 3.– Cold-wall convective, q_{ocw}, and radiative, q_R, heat loadings at a near-stagnation body point.

Figure 3 shows the assigned cold-wall convective and the radiative heat loadings as functions of time for the body point being calculated. These loadings obtained from the private communication noted above had been evaluated by using the equivalents of equations (62), (72), and (79). The heating-rate distributions over the surface were mainly based on wind-tunnel tests of the model at angles of attack.

The calculated heat-shield response to the assigned loadings is illustrated in figures 4 through 7. In figure 4, typical calculated results show the variation with time of surface recession, χ, and the sum of surface recession and depths of degradation of material (to 90 percent degraded, J = 0.10, and also further back to only 10-percent degraded, J = 0.90). In the latter stages of the flight, the heat loading has decreased (fig. 3) and the surface recession has virtually ended, but interior degradation of material continues at a slow rate because of the slow falling off of the internal temperature.

Figure 5 shows the rate of mass loss due to pyrolysis, $\dot{m}_{gw}$, and that due to surface recession, $\dot{m}_{surface} = \dot{m}_{chcomb} + \dot{m}_{chero} + \dot{m}_{chsub}$. Most of the material lost in this flight is due to pyrolysis. The loss proportion between pyrolysis and surface loss is partly determined by the properties of the material; in particular, it is known that with degradation some materials produce more char than other ablating materials.

Figure 6 shows the calculated values of temperature at the

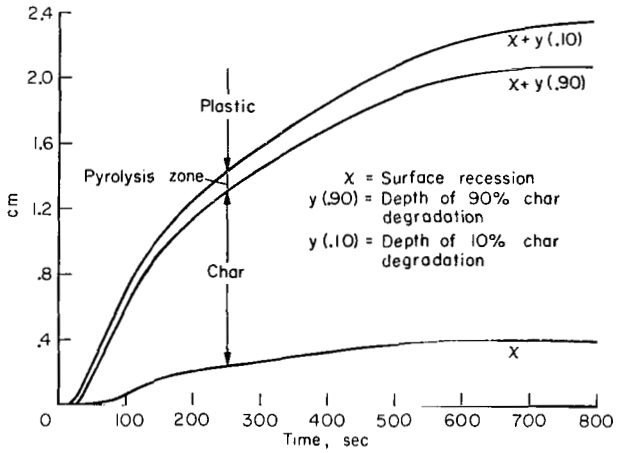

Figure 4.– Calculated heat-shield response; surface recession and depth of degradation.

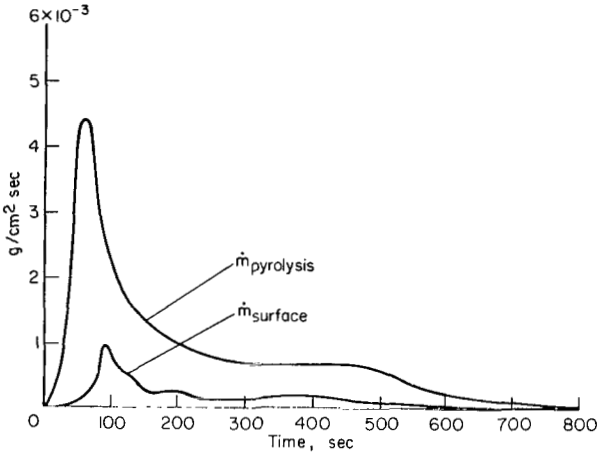

Figure 5.– Calculated heat-shield response; mass loss rates.

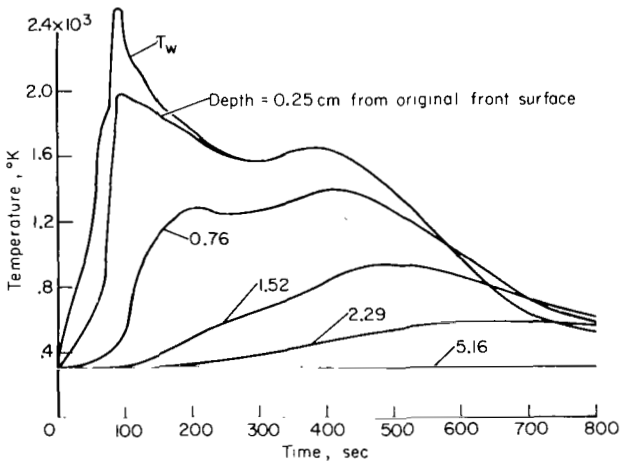

Figure 6.– Calculated heat-shield temperatures.

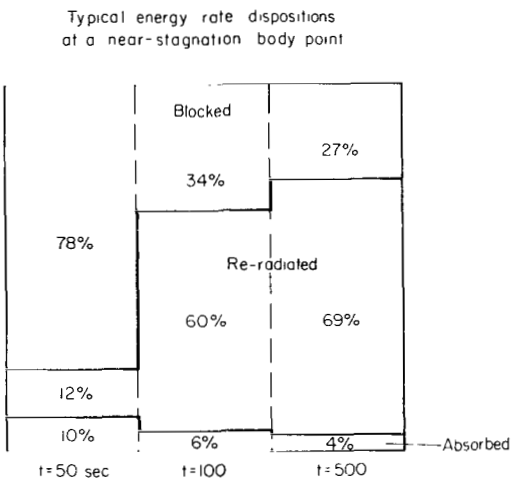

Figure 7.– Calculated energy rate dispositions.

surface and at several fixed points in the interior of the material. There is a time lag of temperature rise with depth in the material, as would be expected. During the latter stages of the flight, the surface is actually undergoing cooling, and the highest temperatures are then in the interior. The curve for a depth of 0.25 cm ends when surface recession reaches that depth. For any given time, one can use figure 4 to determine the state of degradation at each of the fixed depths for which temperatures are plotted in figure 6.

Figure 7 shows typical energy-rate dispositions for three selected times in the flight. At 50 seconds, the loading is moderate (and increasing), as in figure 3. Most of the energy loading is accounted for by blockage. Pyrolysis is occurring (fig. 5), but the surface temperature is still low (fig. 6), so there is relatively little radiation. At 100 seconds, the loading is near the

maximum (fig. 3), and most of the energy is accounted for by re-radiation because the surface temperature is high (fig. 6). Blockage accounts for about one-third of the energy input, a relative decrease from that at 50 seconds. In energy units, cal $cm^{-2}sec^{-1}$, however, this blockage is about 50 percent higher than that at 50 seconds; the pyrolysis rate is greater (fig. 5), and there is more convective heat loading to be blocked. At 500 seconds the relative energy dispositions are only slightly shifted from the proportions at 100 seconds. The main effect here is that the loading has become small (fig. 3). The pyrolysis rate is low (fig. 5), so that the blocked energy magnitude is small, and the re-radiation is also small because of the low surface temperature (fig. 6).

An approximate measure of the ablator efficiency is the smallness of the absorbed energy term as this is the only energy that actually gets into the ablator. This energy is mainly accounted for by the pyrolysis, heating up, and loss of gaseous material, and to a lesser extent by the heating up and loss of solid material from the surface. A very small amount of the energy absorbed is also accounted for by storage of sensible heat in the ablator. (Over the entire flight the total sum of this energy becomes almost negligible because of the cooling at the end of the flight.)

A sublimation energy term was (routinely) calculated, but it is negligible for this flight because of the range of surface temperatures. Sublimation with a charring ablator can be important, and even dominant, for higher speed flights such as from planetary returns. Sublimation involves a loss of charring material at the surface with the removal of energy at the surface.

DISCUSSION AND CONCLUSIONS

A general method has been presented for determining the response in the stagnation region of the charring ablator type of heat shield. The analysis given is actually for an axisymmetric blunt-body stagnation point, but calculations obtained from the analysis form a good approximation for the stagnation region of any arbitrary blunt body when the heat loading can be evaluated for the point at which the calculations are made. An even more approximate use of the calculations can be made for body points far from the stagnation region. This is considered acceptable when these points have relatively low loadings. The calculations can be performed for a variety of conditions, such as for wind-tunnel tests or flight cases; the heat loadings can be calculated by the computing programs, or the loadings can be arbitrarily assigned as functions of time. Properties of the heat-shield material can be arbitrarily assigned.

The important use of the analysis and the associated computing programs is to calculate the performance of heat shields for flight. For any given heat-shield material, it is highly desirable to have comparisons of calculated heat-shield performance with results from a range of experimental tests in wind tunnels. Comparisons with experiment are important, because the effective physical and thermodynamic properties of a material that is being used as a

charring ablator may not be completely known. When these comparisons are good, one can have confidence that the properties of the heat-shield material are being adequately represented in the calculations, and predictions of heat-shield performance for flight cases should be satisfactory.

Since heat shields have a finite depth, the most rigorous method of calculation is the finite depth formulation with an appropriate back boundary condition. The semi-infinite type of calculation is faster and simpler. It is virtually as accurate if there is a safety factor of sufficient material such that there is virgin plastic remaining at the conclusion of the flight or test. This is the case because the events of importance occur near the front surface where temperatures can be an order of magnitude higher than at the back. One can generally say that, if it is necessary to use a finite depth calculation to represent the physical situation, the initial depth or initial amount of heat-shield material is probably marginal.

Numerical calculations are carried out by means of a family of computing programs. The selection of programs and the options within the programs are described in appendix C. This appendix gives detailed instructions in the use of the programs, and it contains a sample case for illustration. The programs can be obtained from COSMIC, University of Georgia, Athens, Georgia, 30601.

Ames Research Center
National Aeronautics and Space Administration
Moffett Field, Calif., 94035, June 22, 1970

APPENDIX A

PRINCIPAL NOMENCLATURE

In performing computer calculations, some purely FORTRAN quantities are used in the input data which have no counterpart among the symbols listed below. These quantities are in appendix C, wherein all FORTRAN quantities are listed and identified.

A	frontal area of vehicle, cm^2
A_{cq}, A_{cv}	free-molecule accommodation coefficients for heat transfer and sublimation mass loss, respectively, dimensionless
A_1	constant defined by equation (54)
A_3	constant defined by equation (75)
A_4	constant defined by equation (62)
A_5	constant defined by equation (77a)
B	blowing parameter defined by equation (76a), dimensionless
c_{ch}, c_p, c_s	specific heat of char, virgin plastic, solid material (virgin plastic to char), respectively, cal/g °K (see eq. (13))
c_{pg}	specific heat of pyrolysis gas at constant pressure, cal/g °K
$\overline{c}$	heat capacity per unit area of backing material, cal/cm^2 °K (eq. (87c))
$\overline{c}_p$	average specific heat, external gas, cal/g °K; defined by equation (57a)
C_D, C_{DC}, C_{DFM}	drag coefficient, dimensionless; drag coefficient, continuum; drag coefficient, free molecule
C_E	Arrhenius activation temperature for surface combustion, °K (eq. (35))
C_J	modification factor for thermal conductivity in pyrolysis zone, dimensionless (eq. (14))
C_{kdb}	reciprocal of mass ratio of carbon/char, dimensionless (eq. (43))
C_{ox}	mass fraction of oxygen in ambient gas, dimensionless (eq. (26))

C_{oxf}	mass fraction of oxygen (dimensionless) at outer edge of boundary layer after depletion by homogeneous combustion (eq. (30))
C_{oxw}	mass fraction of oxygen (dimensionless) at the wall (eqs. (31)-(33), (36)-(41))
C_x	stoichiometric ratio of oxygen to carbon (by weight) in the surface combustion reaction, dimensionless (eqs. (43)-(45))
$C_\psi, C_{\psi_2}, C_{\psi_3}$	constants defined in equation (77)
C_1, C_2	constants in nose radius (eq. (60))
C_3, C_4	constants in M/A (eqs. (92), (95))
C_6	constant vorticity correction in equation (62)
d	damping coefficient (general), dimensionless (eq. (112))
D	free-stream density, g/m^3
e	error in energy rate balance, defined by equation (105)
E_2	stoichiometric ratio (by weight) of oxygen/pyrolysis gas for the homogeneous combustion reaction assumed, dimensionless (eq. (27))
E_3	constant in average specific heat of external gas (eq. (57b))
E_4, E_5, E_6	constants in gas-cap radiation (eq. (79))
E_7	constant to account for shift of sublimation equilibrium (eq. (50))
E_8	constant in vapor pressure (eq. (49))
E_9	constant defined by equation (94)
E_{10}	constant in average specific heat of external gas (eq. (57b))
E_{12}	average ambient enthalpy, km^2/sec^2 (eq. (91))
E_{13}	constant depending on body shape and flight conditions in the drag calculation (eqs. (93), (95))
E_{16}	constant used in tumbling correction (eq. (61))
E_{17}	constant in nose radius (eq. (60))

E_{18} constant in M/A (eqs. (92), (95))

E_{19} constant in vapor pressure (eq. (49))

$\dot{E}_{ff}$ rate of energy liberation at flame front from homogeneous combustion, cal/cm^2sec (eq. (82))

F_e, F_w dimensionless stream function at outer edge of boundary layer and at wall, respectively (see appendix B, eqs. (B1)-(B7))

g_{pl} gravitational acceleration of planet, cm/sec^2 (eq. (89b))

h enthalpy, cal/g

h_g enthalpy of pyrolysis gas, cal/g (eq. (99))

h_{gc} energy liberated by combustion of a unit mass of pyrolysis gas, cal/g

h_{gce} effective energy of combustion per unit mass of pyrolysis gas, cal/g (defined by eq. (81))

h_s enthalpy of solid material, cal/g (eq. (98))

h_{scomb} energy liberated by combustion of a unit mass of char, cal/g (eq. (85))

h_{sero} energy liberated by removal of a unit mass of char by means other than combustion or sublimation (called erosion), cal/g (eq. (85))

h_{sr} energy released by pyrolysis reaction per unit mass of gas produced, cal/g; negative for endothermic reactions; used in equation (1); generally a function of temperature, and can be approximated as $h_{sr} = (\rho_p h_p - \rho_{ch} h_{ch})/(\rho_p - \rho_{ch}) - h_g$; can also be approximated as a constant; see h_{sref} below

h_{sref} a constant; same as h_{sr} if h_{sr} is approximated as constant; also used to evaluate h_g (eq. (99)); when h_{sr} is made temperature dependent as in equation (99), h_{sref} is a reference h_{sr} at a reference temperature (usually $0^\circ K$); FORTRAN symbol, HSREF; cal/g

h_{st} stagnation enthalpy, cal/g

h_{sub} energy absorbed by removal of a unit mass of char by sublimation (positive value), cal/g (eq. (86))

h_∞ free-stream enthalpy, cal/g

$\overline{h}$ enthalpy of interior material, solid and gaseous, per unit area per unit depth, cal/cm^3 (eq. (100))

$\overline{h}_T$ stored energy (enthalpy) of interior material, solid and gaseous, per unit area, cal/cm^2 (eq. (101))

j order of surface combustion reaction, dimensionless (eq. (36))

J measure of degradation defined by equation (7), dimensionless; J = 1 represents virgin plastic; J = 0 represents pure char

K Arrhenius rate for pyrolysis reaction; defined in equations (4), (5)

K_d oxygen diffusion rate constant; defined in equation (32)

K_{ox} Arrhenius reaction rate of oxygen consumption in surface combustion; defined by equation (35)

K_r Arrhenius frequency factor (constant) in K_{ox} (eq. (35))

K_{re} defined by equation (40)

K_1 constant, read in (CK1); defined by equation (38) (see also eqs. (39), (40))

K_2 constant, read in (CK2); modifies char erosion rate, dimensionless (see eq. (46) and following discussion)

$\overline{K}$ fractional time that calculated point is initially exposed to approximately stagnation conditions, dimensionless; for tumbling correction, equation (61)

$\overline{K}_{tu}$ heat-transfer tumbling correction, dimensionless (eq. (61))

$\overline{K}_{-1}$ same as K, but for the preceding time line and spaced according to the $\overline{y}_{-1}$ array (used in eq. (12))

$\overline{\overline{K}}_{ch}, \overline{\overline{K}}_p, \overline{\overline{K}}_s$ coefficient of thermal conductivity of char, virgin plastic, solid material (virgin plastic to char), respectively, cal/cm sec °K (eq. (14))

Le Lewis number, dimensionless

$\frac{L}{\overline{Dr}}$ lift/drag ratio, dimensionless

m exponent in erosion rate calculation, dimensionless (eq. (46))

$\dot{m}_c$ rate of mass loss that contributes to convective heat blockage, g/cm^{2}sec (eq. (75)); ($\geq$ 0)

$\dot{m}_{chcomb}, \dot{m}_{chcomb_{d\ max}}, \dot{m}_{chcomb_{r\ max}}$	rate of char loss by combustion, maximum rate by oxygen diffusion, maximum chemical reaction rate, respectively; g/cm^2sec (eqs. (43), (44), (45)); (≥ 0)
$\dot{m}_{chero}$	rate of char loss by means other than combustion or sublimation (called erosion), g/cm^2sec (eq. (46)); (≥ 0)
$\dot{m}_{chsub}, \dot{m}_{chsFM}, \dot{m}_{chsd}$	rate of char loss by sublimation, free-molecule rate, diffusion rate, respectively; g/cm^2sec (eqs. (53), (48), (52)); (≥ 0)
$\dot{m}_g$	rate of flow of pyrolysis gas past a point in the material, g/cm^2sec (eqs. (20b), (21c)) (≥ 0)
$\dot{m}_{gw}$	$\dot{m}_g$ at the surface (pyrolysis gas expelled), g/cm^2sec
$\dot{m}_{surface}$	$\dot{m}_{chcomb} + \dot{m}_{chero} + \dot{m}_{chsub}$, g/cm^2sec
$\dot{m}_T$	total mass loss rate of material, g/cm^2sec (eqs. (74a,b))
M	mass of vehicle, g; also grid point number in finite difference computation
M_{cv}	molecular weight of char sublimation vapor, g/mole (eqs. (47), (48), (52))
M_g	molecular weight of pyrolysis gas, g/mole (eq. (15))
M_p	molecular weight of gaseous products after heterogeneous combustion, g/mole (eq. (77a))
M_T	total mass loss of material, g/cm^2 (eq. (74c))
n	order of pyrolysis reaction, dimensionless (eq. (4))
p	pressure, $dynes/cm^2$ or atm, as specified
p_{s_2}	external pressure, $dynes/cm^2$ (eq. (15))
p_{t_2}	pressure downstream of normal shock, atm
p_{ve}	equilibrium vapor pressure of char sublimation vapor, atm (eq. (49))
p_{vm}	modified equilibrium vapor pressure of char sublimation vapor, atm (eq. (50))
p_w	external pressure, atm

P ratio of pressure of external gas to modified equilibrium vapor pressure of char sublimation vapor, dimensionless (eq. (51))

Por porosity of char, dimensionless (eq. (17c))

q heat-transfer rate, cal/cm^{2}sec; all surface heat-transfer terms are positive into the material

The following are front surface convective heat-transfer rates, cal/cm^{2}sec:

q_{FM} free-molecule rate (eq. (64))

q_{ocw} cold wall rate (eq. (72))

q_{oc} continuum rate with no blowing (eq. (62))

q_{oo} no blowing rate, bridged between q_{FM} and q_{oc} (eq. (67))

q_o q_{oo} corrected for tumbling or oscillation (eq. (68))

$q_{\psi c}$ continuum rate with blowing (eq. (63))

$q_{\psi w}$ with blowing, bridged between q_{FM} and $q_{\psi c}$ (eqs. (65), (69b))

q_w $q_{\psi w}$ corrected for tumbling or oscillation (eqs. (66), (70))

The following are surface heat-transfer rates (other than front surface convective), cal/cm^{2}sec:

q_{BF} heat-transfer rate into back surface (usually by conduction) (eq. (87b))

q_{cg} front surface heat-transfer rate due to homogeneous combustion (eq. (84))

q_{cs} front surface heat-transfer rate from heterogeneous combustion and erosion (eq. (85))

q'_{cs} front surface heat-transfer rate due to heterogeneous combustion only (eq. (115))

q_R gas cap radiation rate into front surface (eq. (79))

q_{rad} net radiative heating rate into front surface (eq. (80))

q_{sub} heating rate into front surface due to sublimation (eq. (86))

q_{wri} combined initial convective and radiative heating rate into front surface (eq. (124))

The following energy rate terms are not surface heat-transfer rates. They appear in the energy rate balance equation (104), along with the appropriate surface heat-transfer rate terms; cal/cm^{2}sec.

q_{res} — residual in energy rate balance (eq. (104))

q_{stor} — rate of increase of stored energy in the material (eq. (102))

q_{vcon} — convective energy rate of solid and gaseous material, positive out of control volume; it is the energy taken in to heat up and degrade the material (eq. (103))

The following energy terms are time integrals of the corresponding q values; they appear in the cumulative energy balance equation (107).

$Q_w, Q_{BF}, Q_{cg}, Q_{cs}, Q_{rad}, Q_{sub}, Q_{stor}, Q_{vcon}$ — cal/cm^2 (eq. (106))

Q_{res} — residual in cumulative energy balance, cal/cm^2 (eq. (107))

R — effective nose radius, cm (may be fictitious for off-stagnation approximate calculations)

R_{air} — gas constant for external (ambient) gas, atm cm^3/g °K (used only in eqs. (37), (38))

R_g — universal gas constant, ergs/mole °K

R_{pl} — planet radius, km (eq. (89))

S_h — atmosphere scale height, km (eq. (90))

S_{h_i} — initial scale height for entry into an arbitrary atmosphere, km (eq. (133) and contained in eq. (137))

$S_{h_1}, S_{h_2}, S_{h_3}$ — successive scale heights in an arbitrary atmosphere, km:

$S_h = S_{h_1}$ when $\overline{\rho}_\infty \leq \overline{\rho}_{\infty_2}$

$S_h = S_{h_2}$ when $\overline{\rho}_{\infty_2} < \overline{\rho}_\infty \leq \overline{\rho}_{\infty_3}$

$S_h = S_{h_3}$ when $\overline{\rho}_\infty > \overline{\rho}_{\infty_3}$

S_p — frequency factor for Arrhenius rate constant, K, for pyrolysis reaction (eq. (5))

t — time, sec

t_{off} — time, t, at which external loading is set to zero in computing programs; shut off time for wind-tunnel cases with calculated loadings; for flight cases or arbitrarily programmed loadings, should be made larger than any time considered, sec

T — temperature, °K

T_o — initial temperature deep in material, °K (eq. (122))

T_{ref} — reference temperature, °K; may be used in material properties subprograms; generally zero

T_w — wall (front face) temperature, °K

T_{wc} — corrected wall temperature, °K (see discussion following eq. (119))

T_{wp} — predicted wall temperature, °K (eq. (119))

$\overline{T}_{-1}$ — temperature array of preceding time line based on the $\overline{y}_{-1}$ array; used to calculate $\overline{K}_{-1}$ array; °K

u — horizontal component of trajectory velocity, km/sec (eqs. (88), (89))

u_e — tangential velocity at outer edge of boundary layer, cm/sec (eqs. (B1)-(B3))

v — vertical component of trajectory velocity (positive upward), km/sec (eqs. (88)-(90)); also normal velocity in boundary layer as used in appendix B, cm/sec

v_{air} — velocity of external (ambient) gas normal to front surface and considered positive, cm/sec (eqs. (24),(25))

$\overline{v}_s$ — velocity of solid material in coordinate system (y direction), cm/sec; $|\overline{v}_s|$ = rate of surface recession (eq. (2))

$\overline{v}_{s\,comb}, \overline{v}_{s\,ero}, \overline{v}_{s\,sub}$ — $\overline{v}_s$ due respectively to combustion, erosion, sublimation; cm/sec (eq. (2))

$\overline{\overline{v}}_g$ — volume occupied by pyrolysis gas per unit spatial volume, dimensionless (eqs. (15), (17))

V — enthalpy velocity, km/sec; defined as $V^2 = 0.00836h_{st}$ (eq. (56))

V_∞ — free-stream (trajectory) velocity, km/sec (eq. (88a))

$\dot{w}_g$	rate of pyrolysis, from solid to gas per unit space volume, g/cm^3sec (eqs. (3), (4))
x	longitudinal coordinate along meridian (in boundary layer), cm (eqs. (B1)-(B3))
y	coordinate normal to front surface (inward), cm
y(0.10)	depth of 10-percent char degradation (J = 0.90), cm
y(0.90)	depth of 90-percent char degradation (J = 0.10), cm
$\overline{y}_{-1}$	array of y values from the preceding time line, referring to the same points in the material as the current y array; deeper than the y array by the increase in surface recession between the two time lines; $\overline{y}_{-1}(M) = y(M) + \Delta\chi$, cm (see discussion following eq. (11))
z	array defined by equation (9)
$\overline{z}_{-1}$	array, same as z, but for the preceding time line and spaced according to the $\overline{y}_{-1}$ array (used in eq. (12))
Z_x	stability parameter for finite differencing, dimensionless; defined by equation (111); should be $\leq 1/2$.
$\alpha_1, \alpha_2, \alpha_3, \alpha_4$	constants in equation (46)
γ	trajectory angle, deg; positive above horizontal (eq. (88b))
Δ	thermal thickness, defined by equation (96), cm; also increment, for example, Δh = enthalpy potential, cal/g
Δ_{V^2}	increment of enthalpy potential due to homogeneous combustion (eq. (83)); in V^2 units; km^2/sec^2
ε	surface emissivity, dimensionless (eq. (80))
θ_p	activation temperature for the Arrhenius rate, K, for the pyrolysis reaction, °K (eq. (5))
μ	viscosity, poise (eqs. (B1)-(B7))
ρ	density, g/cm^3

$\rho_p, \rho_{ch}, \rho_{cha}, \rho_g, \rho_s$ — densities, g/cm^3; virgin plastic, pure char based on total spatial volume (includes volume occupied by gas), pure char based on volume occupied by solid particles of char only (eqs. (16), (17)), gas based on spatial volume (eq. (15)), solid (based on spatial volume) which can vary between ρ_{ch} and ρ_p (eqs. (7), (11))

$\overline{\rho}_\infty$ — free-stream atmospheric density in Earth sea-level atmospheres, dimensionless, D/1226

$\overline{\rho}_{\infty_2}, \overline{\rho}_{\infty_3}$ — values assigned to $\overline{\rho}_\infty$ at which changes of scale height in an arbitrary atmosphere occur; see S_{h_1}, S_{h_2}, S_{h_3}

σ — Stefan constant, 1.369×10^{-12} cal/cm^{2}sec °K^4 (eq. (80))

ϕ — approximation of the ratio of stored energy to the stored energy associated with an exponential temperature profile, dimensionless (eq. (97))

$\overline{\phi}$ — constant, dimensionless (defined by eq. (B7))

χ — surface recession, cm

χ_1 — characteristic recession depth, cm, used in tumbling correction (eq. (61))

ψ — convective heat blockage factor, dimensionless (eq. (78))

$\overline{\psi}$ — modified convective heat blockage factor, dimensionless (eq. (71))

Subscripts

Subscripts listed below should be referred to when a subscripted symbol is not listed in the nomenclature above. Subscripts can be combined.

air — external gas or air

BF — back face

c — continuum; also corrected

c' — as defined by equation (113)

calc — calculated

ch — char

comb — combustion

d	diffusion
e	outer edge of boundary layer; also quantity based on energy balance
ero	erosion (other than combustion or sublimation)
ex	excess
FM	free molecule
g	pyrolysis gas
i	initial
L2,L3,L4	refer to the second, third, and fourth finite difference calculated grid points; used in equations (117), (120); see appendix C, sketch (h)
M,N	index numbers
max	maximum
MF	in semi-infinite calculations, refers to greatest depth considered (same as BF); in finite depth calculations refers to a virtual point (whose depth may be greater than the BF point); see Numerical Analysis and Computation Procedures, Some Features of the Computer Program, Back Boundary Condition and appendix C, sketch (h)
o	no blowing
ox	oxygen
p	virgin plastic; also predicted
r	reaction
s	refers to solid ablating material (which can vary from virgin plastic to pure char)
st	stagnation
sub	sublimation
theo	theoretical
w	wall (front face)
1	dummy variable

-1 previous time line

∞ free stream

Superscript

$(\dot{})$ time derivative

APPENDIX B

CALCULATION OF AIR FLOW FOR OXYGEN DIFFUSION

The amount of oxygen that can diffuse to the solid surface to support heterogeneous combustion depends originally on the availability of oxygen which, in turn, depends on the rate of air flow into a control volume. We take the outer edge of the control volume to be at the assumed flame front for homogeneous combustion. The homogeneous combustion causes some depletion of oxygen, and it is necessary to calculate a corrected concentration of oxygen at this location which then (less the surface concentration) becomes the driving potential for diffusion of oxygen to the surface. We use a Lewis analogy for the rate of oxygen diffusion, so we want the corrected concentration of oxygen to be evaluated where we evaluate the enthalpy for the enthalpy potential, the "outer edge" of the boundary layer.

From boundary-layer theory and an integration of the continuity equation, we obtain

$$(\rho v)_e - (\rho v)_w = \sqrt{2(\rho\mu)_w \left(\frac{du_e}{dx}\right)_{x=o}} (F_e - F_w) \tag{B1}$$

where v is considered positive in the direction of the surface, and F is the standard dimensionless stream function as defined in reference 12. Equation (B1) corresponds with equation (6.14) of reference 12 when there is no mass transfer at the surface. Equation (B1) is rewritten

$$(\rho v)_e - (\rho v)_w = \sqrt{\frac{(\rho\mu)_w}{(\rho\mu)_{st}}} \sqrt{2(\rho\mu)_{st}\left(\frac{du_e}{dx}\right)_{x=o}} (F_e - F_w) \tag{B2}$$

A modified Newtonian approximation is used for the gradient of u_e:

$$\left(\frac{du_e}{dx}\right)_{x=o} \approx \frac{C_A}{R}\sqrt{\frac{2p_{t_2}}{\rho_{st}}} \tag{B3}$$

where the constant C_A allows p_{t_2} to be evaluated in atmospheres. We evaluate ρ_{st} with the perfect gas law in terms of p_{t_2} and T_{st} and approximate the viscosity as

$$\mu_{st} = C_B T_{st}^{1/2} \tag{B4}$$

When we evaluate constants for air, we have:

$$(\rho v)_e - (\rho v)_w = 0.1566\sqrt{\frac{(\rho\mu)_w}{(\rho\mu)_{st}}}\sqrt{\frac{p_{t_2}}{R}}\,(F_e - F_w) \tag{B5}$$

The second terms on both sides of equation (B5) should be equal. This is also indicated by equation (6.14) of reference 12, which is written for any position in the boundary layer. Accordingly,

$$(\rho v)_e = 0.1566\sqrt{\frac{(\rho\mu)_w}{(\rho\mu)_{st}}}\sqrt{\frac{p_{t_2}}{R}}\;F_e \tag{B6}$$

Equation (B6) can also be obtained directly from equation (6.14) of reference 12. The value of F_e is not overly sensitive to variations in F_w. This is shown in an extended (unpublished) version of reference 13, and is also indicated in reference 14. Analysis of results for air presented in reference 12 indicates that for a relatively cold wall, the product, $\sqrt{(\rho\mu)_w/(\rho\mu)_{st}}\;F_e$, is rather insensitive to a variation in wall enthalpy, and for air it has a value of about 2.95. For convenience, we will define

$$\overline{\phi} = \frac{\sqrt{\frac{(\rho\mu)_w}{(\rho\mu)_{st}}}\,F_e}{2.95} \tag{B7}$$

Then equation (B6) becomes:

$$\dot{m}_{\substack{air\\calc}} = (\rho_{air} v_{air})_{\substack{e\\calc}} = 0.462\overline{\phi}\sqrt{\frac{p_{t_2}}{R}} \tag{24b}$$

where we have changed the subscript on ρv to e_{calc} in equation (24b). In the absence of other data, $\overline{\phi}$ is normally unity. For oxygen-containing gases other than air, $\overline{\phi}$ may be adjusted because the constant, 0.1566, in equations (B5) and (B6) applies to air. The evaluation of the external gas (air) flow obtained from equation (24b) is always compared with the evaluation from equation (24a), and the lesser value is used for the rate of air flow as given by equation (25).

The purpose of the calculation described is to obtain the oxygen concentration after some degree of depletion by homogeneous combustion. Clearly, there is some uncertainty in the calculation, because we are working with the "outer edge" of the boundary layer. In general, this uncertainty is not critical. We can rewrite equation (30) by combining into it equations (26),

(27), and (28) and obtain

$$C_{oxf} = C_{ox} - \frac{\dot{m}_{gw} E_2}{\dot{m}_{air}} \tag{B8}$$

For moderate rates of gas expulsion, $\dot{m}_{gw}$, an error in $\dot{m}_{air}$ can make a smaller relative error in C_{oxf}. For larger rates of gas expulsion, the relative error in C_{oxf} need not be small, but C_{oxf} will be small, and there will be little heterogeneous combustion anyway. As shown in equation (29), C_{oxf} is assigned the value zero, when the apparent calculated value from equation (B8) is negative. This occurs at the largest $\dot{m}_{gw}$ values, and then an error in $\dot{m}_{air}$ is of no consequence for heterogeneous combustion. The value of unity for $\overline{\phi}$ in equation (24b) appears to be valid for ablation in air. It gives results that are consistent with data reported in figure 11 of reference 13.

APPENDIX C

USE OF COMPUTING PROGRAMS

The computing program is actually a group of programs for handling several types of problems. Two of the main programs accept arbitrary heating rates, one of these programs being for a semi-infinite depth material while the other is for a finite depth material (with a back boundary condition applied). Two other main programs (finite and semi-infinite) use heating rates that are calculated in the programs themselves. A fifth main program is a continuation of the semi-infinite arbitrary heating-rate program which allows a calculation to be interrupted and resumed (with possibly a new grid spacing). The continuation program need not be a continuation of any previous calculations. It allows one to read in arbitrary initial conditions including temperature and degradation profiles, $T_i(y)$ and $J_i(y)$, and rate of gas generation, $\dot{m}_{gi}(y)$. The main programs can be used for either wind-tunnel or flight calculations.

Subprograms are used with each main program as indicated by the groupings below.

Main Programs

Main A	Arbitrary Q, semi-infinite
Main B	Arbitrary Q, semi-infinite, continuation
Main C	Arbitrary Q, finite
Main D	Aerodynamic Q, semi-infinite
Main E	Aerodynamic Q, finite

Starting Values Subprograms

Subprogram SV1	Starting values, arbitrary Q
Subprogram SV2	Starting values, aerodynamic Q

Front Surface Subprograms

Subprogram FSEB1	Front surface energy balance, arbitrary Q
Subprogram FSEB2	Front surface energy balance, aerodynamic Q

Back Surface Subprogram (Typical)

Subprogram QBACK	Back surface energy balance, finite heat sink

Trajectory Subprogram

Subprogram DER	Trajectory equations, aerodynamic Q

Printing Subprograms (Typical)

Subprogram PRINTSI	Print, semi-infinite
Subprogram PRINTF	Print, finite

Material Properties Subprograms (Typical)

Subprogram ALPROPA	Material properties, Apollo-type material, j = 0.5
Subprogram ALPROPB	Material properties, high-density phenolic nylon material, j = 0.5
Subprogram ALPROPC	Material properties, same as ALPROPB except j = read in (B13)

The starting values and front surface subprograms are selected to go with a main program of either the arbitrary heating-rate type or the aerodynamically calculated heating-rate type. The back surface subprogram is used only with main programs for finite depth, C and E. The trajectory subprogram is used only for aerodynamic heating cases (main programs D and E) and is then only needed for flight cases. The printing subprograms go with semi-infinite calculations (main programs A, B, D) or finite calculations (main programs C and E). The material properties subprogram is selected to correspond to the ablation material being used. For some new type of material, it may be necessary to write a new material properties subprogram, but this is easily done. Within the grouping of main and subprograms listed above, there are also library-type subroutines that perform such operations as differentiation, integration, and interpolation.

In the program listing above, the back-surface subprogram, the printing subprograms, and the material properties subprograms should be considered as typical; an unlimited number of variations of these subprograms can be written. The back surface subprogram that is listed considers the backing material as a heat sink with an arbitrary finite heat capacity. The program solves equations (87b) and (87c).

Variations in the listed printing subprograms can be made to print out any new quantities desired. For example, by interpolation, one can print out temperatures at fixed positions in the material (say at thermocouple depths). Also, the units of the printed quantities can be changed. These changes involve simple calculations to be performed in the printing subprogram, and they do not affect any of the calculations performed in the main and the other subprograms when new quantities (not in common) are used in the printing subprogram.

In writing a new material properties subprogram, certain quantities must always be determined. The following material properties are generally functions of temperature, T, or they may be constant. These properties are listed as arrays, the index being the grid-point number, M, from 1 to MF + 1. The temperature array of the previous time line T(M) is used to evaluate the temperature-dependent properties. These quantities are: c_p(CPP(M)),

$\int_o^T c_p \, dT_1$(PINT(M)), c_{ch}(CPCH(M)), $\int_o^T c_{ch} \, dT_1$(CHINT(M)), c_{pg}(CPG(M)),

$\int_o^T c_{pg} \, dT_1$(GINT(M)), $\bar{\bar{K}}_p$(CKDBP(M)), $\frac{d\bar{\bar{K}}_p}{dT}$ (DKDBP(M)), $\bar{\bar{K}}_{ch}$(CKDBCH(M)),

$\frac{d\overline{\overline{K}}_{ch}}{dT}$ (DKDBCH(M)), and h_{sr}(HS(M)) (see appendix A). These quantities can be obtained by interpolation of tabular data either read in or put integrally into the beginning of the subprogram (and the tables need not be in common). Or if analytical expressions are available for some of the quantities, they can be evaluated thusly by writing the appropriate equations into the subprogram. Two other arrays are determined in the subprogram, K(CK(M)) and $\overline{K}_{-1}$(CKM1(M)). These can be obtained as functions of arrays of temperatures, T and $\overline{T}_{-1}$ in any way desired, but they are generally calculated by an Arrhenius equation (5), with the constants being read in.

A number of single-valued quantities are determined as functions of surface and external conditions. The quantities associated with heterogeneous combustion are $\dot{m}_{chcomb}$ (F1), equation (43), $\dot{m}_{\substack{chcomb \\ d\ max}}$ (DIRML = VW), equation (44), $\dot{m}_{\substack{chcomb \\ re\ max}}$ (RERML = P), equation (45), and h_{scomb} (HCS), equation (85). The quantity, h_{scomb}, can be calculated as a function of surface temperature, T_w, in this subprogram, but it is often assigned a constant read-in value (HCHREF) in the subprogram. The effective heat of combustion of pyrolysis gases, h_{gce} (HCG) is evaluated in the subprogram according to equation (81), and it thus depends on h_{gc}. This latter quantity can, in principle, be evaluated as a function of boundary-layer temperatures and the extent of oxidation, which will in turn depend on a number of variables. This is clearly not warranted in view of the simple flame front model assumed. The quantity, h_{gc}, is most appropriately put into the subprogram as a read-in constant, HGREF.

The rate of loss of surface material other than by combustion and sublimation (called erosion), $\dot{m}_{chero}$ (F2 = TAUWP), is evaluated in the subprogram. This may be in the form of an empirical expression such as equations (46) or some other evaluation. The energy associated with this process, h_{sero} (CS) is usually zero (see eq. (85)). If h_{sero} is a variable function of surface temperature, say, it should be evaluated in this subprogram. If h_{sero} is a constant, it is read in as CS, and it need not be included in this subprogram.

The loss rates of surface material due to sublimation are calculated in this subprogram. These quantities are $\dot{m}_{chsub}$ (FSUB = UDB(5)), equation (53), $\dot{m}_{chsFM}$ (FSUBRAT = UDB(4)), equation (48), and $\dot{m}_{chsd}$ (FSUBDIF = UDB(6)), equation (52). The energy of sublimation h_{sub} (see eq. (86)) is usually approximated as a constant, in which case it need not be included in the subprogram, but it is read in as E20. If one wishes to make h_{sub} a function of surface temperature, the evaluation should be performed in this subprogram, and for h_{sub}, UDB(2) should be used (which is in common).

Computing Program Options

In addition to the major options determined by selection of a main program and accompanying subprograms, there are several options that can be

selected within the programs:

1. Variation of density of the ablating material
   (a) The solid density, ρ_s, at each depth, y, is not allowed to increase with time. This is only applicable to wind-tunnel conditions with constant heat loading. It is not necessary to use this option. KG = 1.
   (b) The normal situation allows ρ_s to vary freely. (This is valid for wind-tunnel cases also.) KG = 2.

2. Calculation of internal degradation
   (a) The normal calculation follows the degradation of a point in the material. Each point of matter moves in the coordinate system (because of surface recession and because the origin is at the front surface). LL1 = 1.
   (b) An approximate calculation ignores the movement of solid material in the coordinate system. This speeds up computing time and is reasonable when the surface recession is negligibly small. LL1 = 0.

3. Running conditions with aerodynamic heating (main program D or E)
   (a) Normal wind tunnel, KF = 1. No rarefaction effects; uses equation (73).
   (b) Rarefied wind tunnel, KF = 2. Takes account of rarefaction effects, equations (62)-(71). (This includes all wind-tunnel cases, but the computing time is longer than with option (a).) Options (a) and (b) allow the wind tunnel to be shut off if desired; the calculations will continue while the model cools.
   (c) Entry flight with an initial temperature profile in the material that is computed as an exponential profile. With an assumed T_{wi} ($> T_o$), the initial values, D_i and Δ_i, are computed by the program. KF = 3.
   (d) Flight with arbitrary initial values of atmospheric density, D_i, and thermal thickness of an assumed exponential temperature profile in the body, Δ_i. KF = 4.

4. Planet and atmosphere for flight case with aerodynamic heating (main program D or E, with KF = 3 or 4)
   (a) Earth entry with ARDC atmosphere (approximated exponentially with three programmed values of scale height). Earth radius programmed at 6440 km, and $g_{pl} = 980$ cm/sec^2. KC5 = 1.
   (b) Arbitrary planet (R_{pl} and g_{pl}) with exponential atmosphere having arbitrary scale height (initial, two intermediate, and final values). KC5 = 2.

Damping Constants

The damping calculation is given in equation (112). When damping is not used, all damping constants should have the value unity. The read-in quantities, KCT and NOP, are the time-line numbers (N) for the first and second

damping changes, respectively. The tabulation below lists the quantities damped and the first, second, and third damping coefficients.

Quantity	First damping coefficient	Second	Third
T_w	E1	B14	CY
$\dot{m}_g(y, t)$	B6	B7	B6
$\dot{m}_{chcomb}$	B9	B10	B9
$\dot{m}_{chero}$	B11	B12	B11
$\dot{m}_{chsub}$	B11	B12	B11
ψ	PS	CMO	PS

Nomenclature of Computing Program

The nomenclature in the computing program is in symbolic FORTRAN language. Separate listings of input and output data are shown below.

Input Data

Input data are listed below in their order of card punching. Card formats are shown in sketch (g). All input data are printed by the program in an initial readout (see Sample Case, below). A quantity listed as an option is defined in the section, Computing Program Options.

Following the definition of a quantity, certain programs or options may be listed. For other program or option selections, the quantity is not needed or used, but the card formats must be maintained.

The spacing sketch, time sketch, and printing sketch (sketches (h)-(j)) are referred to in the input listings below. The spacing sketch shows the y(M) spacing. The fine-spaced y increments are not used in the finite difference solution of equation (1). After the finite-differenced answers are obtained, the fine increments are used as interpolation points for a closer spacing near the front surface of the printed quantities (e.g., T(M)). See Output Data section.

4	8	12	16	20	24	28	32	36	40	44	48	52	56	60	64	68	72	CARD
KF	KG	N1	N2	NF	K2	K3	K4	LN	M2	M3	MF	J1	J2	KC5	KCT	KM1	KM2	A
KM3	KCM1	KCM2	KCM3	KCMF	KN1	KN2	KCN1	KCN2	KCNF	LL1	NOP	NAR	JJAR	NAROP	JJR2	JJCH		B

ALL NUMBERS IN I4 FORMAT (MUST BE RIGHT JUSTIFIED)

1	10	19	28	37	46	55	64 72	
A1	A2(OPEN)	A3	A4	B1	B2	B3	B4	1
B5	B6	B7	B8	B9	B10	B11	B12	2
B13	B14	B15	B16(OPEN)	C1	C2	C3	C4	3
C5	C6	C7	C8	E1	E2	E3	E4	4
E5	E6	E7	E8	E9	E10	E11	E12	5
E13	E14	E15(OPEN)	E16	SIGMA	RO	OMCO	OKBAR	6
CH11	VCINF1	GAMA1	TW1	DELTW(OPEN)	ALLOW	HST	DC1	7
DDT1	DDT2	DDT3	DY1	RHO21	OMO	E17	E18	8
DELTJ	E19	E20	E21	E22	E23	CJS	CBAR	9
RHOP	RHOCH	RHOCHA	CS	ACT	HSREF	CX	CY	10
A5	A6	CK1	CK2	PS	PT2	CMBW	CMO	11
CMG	PH1BAR	COW	CE	RG	TREF	HCHREF	HGREF	12
CKDB	CMCH(OPEN)	TOFF	E24	E25	E26	E27	E28	13
CO1N	RIN	VCON	QCSIN	QCGIN	QSUBIN	STOR	RESID	14
F1	F2	FSUB	TT	PSI				15
TE(1)	TE(2)	TE(3)	TE(4)	TE(5)	TE(6)	TE(7)	TE(8)	T1
TE(97)	TE(98)	TE(99)						T13
RJ(1)	RJ(2)	RJ(3)	RJ(4)	RJ(5)	RJ(6)	RJ(7)	RJ(8)	R1
RJ(97)	RJ(98)	RJ(99)						R13
CMRGVG(1)	CMRGVG(2)	CMRGVG(3)	CMRGVG(4)	CMRGVG(5)	CMRGVG(6)	CMRGVG(7)	CMRGVG(8)	G1
CMRGVG(97)	CMRGVG(98)	CMRGVG(99)						G13
TTAR(1)	TTAR(2)	TTAR(3)	TTAR(4)	TTAR(5)	TTAR(6)	TTAR(7)	TTAR(8)	A1
TTAR(297)	TTAR(298)	TTAR(299)	TTAR(300)					A38
HSTAR(1)	HSTAR(2)	HSTAR(3)	HSTAR(4)	HSTAR(5)	HSTAR(6)	HSTAR(7)	HSTAR(8)	B1
HSTAR(297)	HSTAR(298)	HSTAR(299)	HSTAR(300)					B38
PT2AR(1)	PT2AR(2)	PT2AR(3)	PT2AR(4)	PT2AR(5)	PT2AR(6)	PT2AR(7)	PT2AR(8)	C1
PT2AR(297)	PT2AR(298)	PT2AR(299)	PT2AR(300)					C38
QOCWAR(1)	QOCWAR(2)	QOCWAR(3)	QOCWAR(4)	QOCWAR(5)	QOCWAR(6)	QOCWAR(7)	QOCWAR(8)	D1
QOCWAR(297)	QOCWAR(298)	QOCWAR(299)	QOCWAR(300)					D38
QRAR(1)	QRAR(2)	QRAR(3)	QRAR(4)	QRAR(5)	QRAR(6)	QRAR(7)	QRAR(8)	E1
QRAR(297)	QRAR(298)	QRAR(299)	QRAR(300)					E38
RAR(1)	RAR(2)	RAR(3)	RAR(4)	RAR(5)	RAR(6)	RAR(7)	RAR(8)	F1
RAR(297)	RAR(298)	RAR(299)	RAR(300)					F38

ALL NUMBERS IN E93 FORMAT (DECIMAL POINT NEEDED)

ALL PROGRAMS

MAIN PROGRAM B

MAIN PROGRAMS A, B, C

Sketch (g).- Input card format.

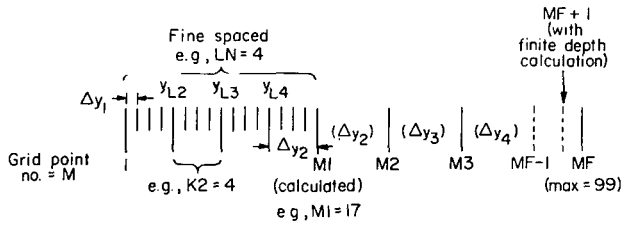

$\Delta y_2, \Delta y_3, \Delta y_4$ are increments used in finite difference equation
Δy_1 = increment used for interpolation

Sketch (h).- Spacing.

N1, N2 are break points for changing Δt

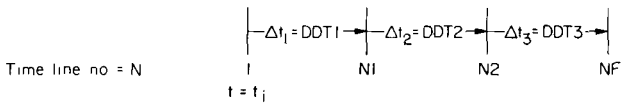

$\Delta t_1, \Delta t_2, \Delta t_3$ are increments used in finite difference equation

Sketch (i).- Time.

One time line
KM1, KM2, KM3 are break points for printing increments

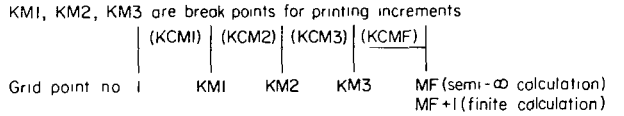

KCM1, KCM2, KCM3, KCMF are grid-point printing increments

Between time lines
KN1, KN2 are break points for printing increments

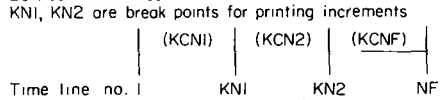

KCN1, KCN2, KCNF are time line printing increments

Sketch (j).- Printing.

Card A
(All numbers are integers in I4 FORMAT)

KF Running condition option, main program D or E

KG Variation of density of the ablating material option

N1 Time-line number at which the finite time increment, Δt, changes from Δt_1 (DDT1) to Δt_2 (DDT2) (see sketch (i))

N2 Time-line number at which the finite time increment, Δt, changes from Δt_2 (DDT2) to Δt_3 (DDT3) (see sketch (i))

NF Final time-line number (see sketch (i))

K2 Defined by $\Delta y_2 = (K2)\Delta y_1$. Can be ≥ 1 (see sketch (h)); Δy_2 is the smallest Δy used in the finite difference equation; quantities in the Δy_1 spacing are obtained by interpolation from the finite-difference obtained values in the Δy_2 spacing.

K3 Defined by $\Delta y_3 = (K3)\Delta y_2$; can be ≥ 1 (see sketch (h))

K4 Defined by $\Delta y_4 = (K4)\Delta y_3$; can be ≥ 1 (see sketch (h))

LN Increments of Δy_2 spacing over which Δy_1 spacing exists; must be ≥ 3 (see sketch (h))

M2 Grid point at which space increment changes from Δy_2 to Δy_3 (see sketch (h)); $(LN)(K2) + 1 = M1 \leq M2 \leq M3$

M3 Grid point at which space increment changes from Δy_3 to Δy_4 (see sketch (h)); $M2 \leq M3 \leq MF$

MF Grid point at deepest point calculated. Maximum value = 99 (see sketch (h)). For semi-infinite calculations (main programs A, B, D), this depth may be greater than actual material depth, and we require $MF \geq M3 \geq M2 \geq M1$. For finite calculations (main programs C, E), this is the initial depth of material; for these cases, we require initially that $MF \geq M3 \geq M2 \geq M1$. Also, if $K2 \neq 1$, require that $MF \geq M1 + 2$ after shrinkage.

J1 Order of interpolation for quantities, $\overline{z}_{-1}(M)$ and $\overline{T}_{-1}(M)$, for previous time line. Used in equation (12). In the computing programs, the value of z is advanced from one time line to the next.

J2 Order of interpolation for calculated temperatures, T, at fine-spaced grid points (see sketch (h))

KC5 Planet and atmosphere option (main program D or E with KF = 3 or 4)

KCT Time line, N, for first damping change

KM1 — Grid point at which printing interval on one time line changes from KCM1 to KCM2 (see sketch (j)); $1 \leq KM1 \leq KM2 - KCM2$

KM2 — Grid point at which printing interval on one time line changes from KCM2 to KCM3 (see sketch (j)); $KM1 + KCM2 \leq KM2 \leq KM3 - KCM3$

Card B
(All numbers are integers in I4 FORMAT)

KM3 — Grid point at which printing interval on one time line changes from KCM3 to KCMF (see sketch (j)); $KM3 \geq KM2 + KCM3$; also $KM3 \leq MF - KCMF$ for main programs A, B, D; $KM3 \leq MF - KCMF - 1$ for main programs C, E (using MF value after shrinkage)

KCM1, KCM2, KCM3, KCMF — Printing intervals of grid points (see sketch (j)) (normally unity)

KN1 — Time-line number at which time-line printing interval changes from KCN1 to KCN2 (see sketch (j))

KN2 — Time-line number at which time-line printing interval changes from KCN2 to KCNF (see sketch (j))

KCN1, KCN2, KCNF — Time-line printing intervals (see sketch (j))

LL1 — Internal degradation option; LL1 = 1, normally

NOP — Time line, N, for second damping change

NAR — Number in loading array; maximum = 300; main programs A, B, and C

JJAR — Initial order of interpolation in loading array; main programs A, B, C

NAROP — Loading array printing option; NAROP = 1, prints array; = 0, does not print; main programs A, B, C

JJR2 — Final order of interpolation in loading array; main programs A, B, C

JJCH — Number in loading array at which order of interpolation changes from initial (JJAR) to final (JJR2); main programs A, B, C

All remaining cards have each number in E9.3 FORMAT, with eight (or fewer) numbers per card.

Card 1

A1 A_1, equation (54); main programs A, B, C; also main programs D, E with KF = 3 or 4

A2 (Open)

A3 A_3, equation (75)

A4 A_4, equation (62), main programs D, E; otherwise, open

B1 $\bar{\bar{K}}_p$ if constant (and unevaluated in the material properties subprogram), otherwise open

B2 $\bar{\bar{K}}_{ch}$ if constant (and unevaluated in the material properties subprogram), otherwise open

B3 S_p, equation (5)

B4 θ_p, equation (5)

Card 2

B5 Should be zero for all cases, except that B5 = t_{off} can be used for constant loading cases (main programs A, B, C and D, E with KF = 1 or 2). B5 $\neq$ 0 is not necessary for these cases, but when $t < B5$, it insures that $K \geq K_{-1}$.

B6 First and third damping coefficients, $\dot{m}_g(y, t)$

B7 Second damping coefficient, $\dot{m}_g(y, t)$

B8 T_o

B9 First and third damping coefficients, $\dot{m}_{chcomb}$

B10 Second damping coefficient, $\dot{m}_{chcomb}$

B11 First and third damping coefficients, $\dot{m}_{chero}$ and $\dot{m}_{chsub}$

B12 Second damping coefficient, $\dot{m}_{chero}$ and $\dot{m}_{chsub}$

Card 3

B13 j, equations (36)-(41), (45). ALPROPC; otherwise open

B14 Second damping coefficient, T_w

B15 ε

B16 (Open)

C1 C_1, equation (60); main programs D, E

C2 C_2, equation (60); main programs D, E

C3 C_3, equations (92), (95); main programs D, E with KF = 3 or 4

C4 C_4, equations (92), (95); main programs D, E with KF = 3 or 4

Card 4

C5 S_{h_1}, equation (90); main programs D, E with KF = 3 or 4 and KC5 = 2

C6 C_6, equation (62); main programs D, E

C7 L/Dr, equation (89); main programs D, E with KF = 3 or 4

C8 $g_{p1} \times 10^{-5}$, equation (89b); main programs D, E with KF = 3 or 4 and KC5 = 2

E1 First damping coefficient, T_w

E2 E_2, equation (27)

E3 E_3, equation (57b)

E4 E_4, equation (79); main programs D, E

Card 5

E5 E_5, equation (79); main programs D, E

E6 E_6, equation (79); main programs D, E

E7 E_7, equations (50), (51)

E8 E_8, equation (49)

E9 E_9, equation (94); main programs D, E with KF = 3 or 4

E10 E_{10}, equation (57b)

E11 M_{cv}, equations (47), (48), (52)

E12 E_{12}, equation (91); main programs A, B, C; also main programs D, E with KF = 3 or 4

Card 6

E13 E_{13}, equations (93), (95); main programs D, E with KF = 3 or 4

E14 A_{cq}, equation (64); main programs D, E with KF = 2, 3, or 4

E15 (Open)

E16 E_{16}, equation (61); main programs D, E with KF = 3 or 4

SIGMA $\sigma = 1.369 \times 10^{-12}$

RO R_i, equation (60); main programs D, E

OMCO $(M/C_{DC}A)_i$, equation (95); main programs D, E with KF = 3 or 4

OKBAR $\overline{K}$, equation (61); main programs D, E with KF = 3 or 4

Card 7

CHI1 χ_1, equation (61); main programs D, E with KF = 3 or 4

VCINFI V_{∞_i}; main programs D, E; for flight cases (KF = 3, 4); for wind-tunnel cases (KF = 1, 2), $V_\infty = V_{\infty_i}$ until $t \geq t_{off}$

GAMAI γ_i; main programs D, E with KF = 3 or 4

TWI T_{wi}; all main programs, but with main program D or E and KF = 3, require $T_{wi} > T_o$

DELTW (Open)

ALLOW n, equation (4)

HST h_{st}; main programs D, E. With KF = 1 or 2 (wind-tunnel case), h_{st} is a constant until $t \geq t_{off}$, when h_{st} becomes zero; for the flight case with arbitrary initial conditions (KF = 4), HST is Δ_i

DCI D_i; main programs D, E; with KF = 1 or 2 (wind-tunnel case), $D = D_i$ = constant until $t \geq t_{off}$ when D becomes zero; for the flight case with arbitrary initial conditions (KF = 4), DCI is D_i

Card 8

DDT1 Δt_1 (see sketch (i))

DDT2 Δt_2 (see sketch (i))

DDT3 Δt_3 (see sketch (i))

DY1 ΔY_1 (see sketch (h))

RHO21 c_{pg} if constant (and unevaluated in the material properties subprogram)

OMO M_{T_i}, equation (74c)

E17 E_{17}, equation (60); main programs D, E

E18 E_{18}, equations (92), (95); main programs D, E with KF = 3 or 4

Card 9

DELTJ R_{pl}, equation (89); main programs D, E with KF = 3 or 4 and KC5 = 2

E19 E_{19}, equation (49)

E20 h_{sub}, equation (86) (positive quantity)

E21 A_{cv}, equations (47), (48)

E22 c_{pwi}; see starting value equations (127), (134), (135), (136); main programs D, E with KF = 1, 2, or 3

E23 $\overline{\overline{K}}_{pwi}$; see starting value equations (123), (127), (136); main programs A, C and main programs D, E with KF = 1, 2, or 3

CJS C_J, equation (14)

CBAR $\overline{c}$, equation (87c), main programs C, E

Card 10

RHOP ρ_p

RHOCH ρ_{ch}

RHOCHA ρ_{cha}

CS h_{sero}, equation (85)

ACT X_i, equation (59); must be read in zero with main program E

HSREF h_{sref}; used to evaluate h_{sr} in the material properties subprogram; negative for an endothermic pyrolysis reaction at a reference temperature (usually 0° K)

CX C_x, equations (43), (44), (45)

CY Third damping coefficient, T_w

Card 11

A5 A_5, equation (77a)

A6 Converts pressure units from atmospheres to dynes/cm^2 = 1.013×10^6

CK1 K_1, equations (38), (39), (40)

CK2 K_2, equation (46)

PS First and third damping coefficients, ψ

PT2 p_{t_2} or p_w, main programs D, E with KF = 1 or 2 (wind-tunnel cases); $^2p_{t_2}$ or p_w is a constant for these cases

CMBW M_p, equation (77a)

CMO Second damping coefficient, ψ

Card 12

CMG M_g, equation (15)

PHIBAR $\overline{\phi}$, equations (24), (B7)

COW C_{ox}, equation (26)

CE C_E, equation (35)

RG R_g, equation (15) (8.317×10^7 ergs mole^{-1} °K^{-1})

TREF T_{ref}, can be used in material properties subprogram (usually zero)

HCHREF h_{scomb} if constant, equation (85); if h_{scomb} is a function of temperature in the material properties subprogram, HCHREF is a reference value of h_{scomb} at some reference temperature

HGREF h_{gc} if constant, equation (81); if h_{gc} is a function of temperature in the material properties subprogram, HGREF is a reference value of h_{gc} at some reference temperature

Card 13

CKDB C_{kdb}, equation (43)

CMCH (Open)

TOFF t_{off}; when $t \geq t_{off}$, V_∞, h_{st}, and D become zero; shut-off time for wind tunnels (main programs A, B, C and D, E with KF = 1 or 2); for flight cases (main programs A, B, C and D, E with KF = 3 or 4), t_{off} must be $\geq$ the flight time

E24 $\overline{\rho}_{\infty_2}$; main programs D, E with KF = 3 or 4 and KC5 = 2

E25 $\overline{\rho}_{\infty_3}$; main programs D, E with KF = 3 or 4 and KC5 = 2

E26 S_{h_2}, equation (90); main programs D, E with KF = 3 or 4 and KC5 = 2

E27 S_{h_3}, equation (90); main programs D, E with KF = 3 or 4 and KC5 = 2

E28 S_{h_i}, equations (132), (133), and contained in equation (137); main programs D, E with KF = 3 and KC5 = 2; has arbitrary value but may equal S_{h_1} (C5)

Cards 14 and 15 and three sets of array cards listed below are used only with main program B (arbitrary Q, semi-infinite, continuation). These additional inputs are initial values that may be arbitrarily assigned or obtained from final values from main program A when a continuation calculation is being made. Cards 14 and 15 and the three sets of array cards ($T_i(y)$, $J_i(y)$, and $\dot{m}_{gi}(y)$) are all in the same format as cards 1 through 13.

Card 14

COIN Q_{wi}, equation (106a)

RIN Q_{radi}, equation (106b)

VCON Q_{vconi}, equation (106g)

QCSIN Q_{csi}, equation (106d)

QCGIN Q_{cgi}, equation (106c)

QSUBIN Q_{subi}, equation (106e)

STOR Q_{stori}, equation (106h)

RESID Q_{resi}, equation (107)

Card 15

F1 $\dot{m}_{chcombi}$, equation (43)

F2 $\dot{m}_{cheroi}$, equation (46)

FSUB $\dot{m}_{chsubi}$, equation (53)

TT t_i

PSI ψ_i, equation (78)

For a continuation calculation, it is also necessary to read in: OMO (M_{T_i}), card 8, equation (74c) and ACT (X_i), card 10, equation (59). Following card 15, the initial temperature array, T_i, is read in: TE (M) on cards T1, T2, . . ., T13. The array of J_i is then read in: RJ (M) on cards R1, R2, . . ., R13. Then the array of $\dot{m}_g$ is read in: CMRGVG (M) on cards G1, G2, . . ., G13. The above three arrays have the dimension, MF, with a maximum value of 99 (up to 13 cards each). The index M of each arrayed quantity corresponds to a depth y (array Y(M)). The spacing of the y array can be selected arbitrarily; it is not necessarily the same as that of prior calculations (when a continuation calculation is being made).

Loading cards are required for main programs A, B, and C. For main program B, the loading cards follow the G1, G2, . . ., G13 cards. For main programs A and C, the loading cards follow card 13. The loading arrays have the dimension, NAR, with a maximum value of 300 (up to 38 cards each), and they are in the same format as cards 1 through 13.

The loading arrays in order are:

Time, t: TTAR (NN) on cards A1, A2, . . ., A38.
Total enthalpy, h_{st}: HSTAR (NN) on cards B1, B2, . . ., B38.
Pressure, p_{t_2} or p_w: PT2AR (NN) on cards C1, C2, . . ., C38.
Cold-wall convective heating rate, q_{ocw}: QOCWAR (NN) on cards D1, D2, . . ., D38.
Radiative heating rate, q_R: QRAR (NN) on cards E1, E2, . . ., E38.
Effective nose radius, R: RAR (NN) on cards F1, F2, . . ., F38.

Output Data

The input data are printed in an initial output format (see Sample Case below). With main programs A, B, and C, the loading data arrays (t, h_{st}, etc.) are printed or not when NAROP is assigned the value 1 or 0. The index number of the loading arrays is also printed (labeled NN).

With main program B, the data read in on cards 14 and 15 are printed out with the first time-line output (always printed). (Some of these numbers may be slightly modified by being recalculated.) The quantities OMO (M_{T_i}) and ACT (X_i) are printed in the initial output, and they are also printed with the

first time-line outputs as TMLO and CHI, respectively. The arrays TE(M), RJ(M), and CMRGVG(M) are printed with the first time-line output.

With all the main programs, the following additional quantities (some calculated) are printed in an initial output (see Sample Case below).

QO1I q_{wi}, equation (124)

QO2I q_{radi}, equation (124)

QOI q_{wri}, equation (124)

TTI t_i; equation (127) with main programs D or E and a wind-tunnel case (KF = 1 or 2). Otherwise, $t_i = 0$ except with main program B (continuation) when TT = t_i is read in.

DELI Δ_i; equation (123) except with main program D or E with KF = 4 (when Δ_i is read in). Δ_i is meaningful with an initial exponential profile (eq. (122)), so it may not be meaningful with the continuation program, main program B.

DCI D_i; with main program D or E and KF = 1, 2, or 4, D_i is read in; with KF = 3, D_i is calculated from equation (137). With main program A, B, or C, D_i is obtained from p_{t_2} and V, equation (54).

RHO $\overline{\rho}_\infty$ = D/1226 (for this printing, D = D_i)

M1 M1 = 1 + (K2)(LN); see sketch (h).

The spacing of printing intervals is arbitrarily selected (see subsection Input Data and sketch (j)). For each time line printed out, the quantities listed below appear. (See subsection, Sample Case, below for format.) The first and last time lines (N = 1 and N = NF) are always printed out.

N N, time-line number

TT t

R R

SNGMA Sin γ

RHO $\overline{\rho}_\infty$

VC V

RERML $\dot{m}_{\substack{chcomb \\ r\ max}}$

PSI ψ

QOFM	q_{FM}
QOC	q_{oc}
QO	q_{o}
QOCW	q_{ocw}
QOO	q_{oo}
DIRML	$\dot{m}_{\substack{chcomb \\ d\ max}}$
QR	q_{r}
DTDYW	$(\partial T/\partial y)_{we}$
OMC	$M/C_{D}A$
TDEL	Δ
CKTU	$\overline{K}_{tu}$
QSUB	q_{sub}
FSUB	$\dot{m}_{chsub}$
F1	$\dot{m}_{chcomb}$
F2	$\dot{m}_{chero}$
TWC	T_{w}
TWCAL	T_{wp}
XIP	$\dot{\chi} = \lvert\overline{v}_{s}\rvert$
CHI	χ
DTT	Δt
FSUBRAT	$\dot{m}_{chsFM}$
FSUBDIF	$\dot{m}_{chsd}$
PHI	ϕ
VCINF	V_{∞}
ABROW	$\dot{m}_{T}$
TMLO	M_{T}
SQOO	$q_{\psi_{w}}$
PT2	p_{t_2} or p_{w}
CHI+YDEG/CH	χ + y(0.90), a depth from original surface
YDEG/PL	y(0.10)
YDEG/CH	y(0.90)
PSIBAR	$\overline{\psi}$
CØIN	Q_{w}
RIN	Q_{rad}
B	B
STOR	Q_{stor}
VCON	Q_{vcon}
CHI+YDEG/PL	χ + y(0.10), a depth from original surface
RESID	Q_{res}
ERR	e
DTDYP	$(\partial T/\partial y)_{\substack{w \\ -1}}$
PSQO	q_{w}
FW	q_{rad}
DTDYR	$(\partial T/\partial y)_{wc}$
DSTOR	q_{stor}
VARG	q_{vcon}
-VSSUB	$-\overline{v}_{ssub}$
DRES	q_{res}
-VSCOMB	$-\overline{v}_{scomb}$

-VSERO $-\overline{v}_{sero}$

QCS q_{cs}

QCG q_{cg}

QCSIN Q_{cs}

QCGIN Q_{cg}

QSUBIN Q_{sub}

The four quantities below are printed out only by subprogram PRINTF (with main program C or E) as these are concerned with finite depth.

QB q_{BF}

QBIN Q_{BF}

DTDYBAK $(\partial T/\partial y)_{BF}$

TEMF T_{MF} (a virtual point)

Also for each time line, the following arrayed quantities are printed out in columns for the selected print spacing of grid points (see sketch (j) and Sample Case below for format).

M M (grid point number)

Y y

TE T

RJ J

RHOS ρ_s

CMRGVG $\dot{m}_g$

XZ Z_x, should be $\leq 1/2$ (for stability)

For semi-infinite depth calculations (subprogram PRINTSI with main program A, B, or D), the last arrayed quantities printed are for grid point number MF. For finite depth calculations (subprogram PRINTF with main program C or E), quantities for grid point number MF are not printed in the columns as MF is a virtual point. Quantities for grid point MF+1 are printed as this point represents the back surface of the material.

Sample Case

The sample case used for illustration is a wind-tunnel case run under the conditions: total enthalpy, h_{st} = 2700 cal/g; free-stream velocity, V_∞ = 3.0488 km/sec; pressure downstream of normal shock, p_{t_2} = 1.04 atm; for a duration of 2 seconds. The model has a hemisphere nose with a radius, R, of 1.905 cm, and is Apollo type heat-shield material. This case could be handled by any of the five main programs; for example, with main program D or E, the loading would be calculated in the program. It was elected, for illustration, to use an arbitrary heating rate main program, so the loading was calculated independently and programmed in as an input. This loading is a cold-wall convective heating rate, q_{ocw} = 226.2 cal $cm^{-2}sec^{-1}$ and a radiative heating rate, q_R, of zero. For further illustration, it was elected to use the continuation type main program B which uses a semi-infinite type calculation, and to start the calculation at a wind-tunnel time, t, of 1 second. The condition of the model at 1 second was previously obtained by use of main program A, and this condition (temperature and extent of degradation as functions of depth, rate of gas generation, extent of surface recession, etc.) furnished inputs to the continuation program. Calculations are for the stagnation point. The programs used for this example are:

Main program B
Starting values subprogram SV1
Front surface subprogram FSEB1
Printing subprogram PRINTSI
Material properties subprogram ALPROPA

The input data for the sample case with proper card formats are shown in figure 8. The print-out of the main part of the input data is given in figure 9. These are the data from cards A through 13 (common to all the main programs). The loading data from cards A1 through F1 are shown (common to main programs A, B, and C), and the initial calculated values are also printed.

The data read in from cards 14 and 15 and the arrays from cards T1-T5, R1-R5, and G1-G5 are peculiar to main program B. These data appear in the print-out of the first time line (N = 1), as shown in figure 10. All subsequent time-line print-outs are in the same format.

```
    5       10      15      20      25      30      35      40      45      50      55      60      65      70  73  CARD  80
          2  41  51 101   6   1   1   4  27  29  39   1   1         21   2   3   A
    4   1   1   1   1  42  58  10  10  10   1  51   4   1   1   1  10          B
1.0         0.0         .5          0.0         0.0         0.0          0.702E811060.           1
0.0         1.0         1.0         311.0       1.0         1.0         1.0         1.0         2
0.0         1.0         .75         0.0         0.0         0.0         0.0         0.0         3
0.0         0.0         0.0         0.0         1.0         1.48        .000084     0.0         4
0.0         0.0         1.0         22.293      0.0         0.1267      33.0        13.31       5
0.0         0.0         0.0         0.0         .1369E-110.0            0.0         0.0         6
0.0         0.0         0.0         311.        0.0         2.0         0.0         0.0         7
.02         .02         .02         .005        0.0         .018802     0.0         0.0         8
0.0         91592.      2696.       1.0         0.0         .0004547    1.0         0.0         9
.5445       .3205       2.25        0.0         .017014     -83.3       1.3333      1.0         10
1.73        1.01300E6280000.        .6          1.0                     15.0        1.0         11
15.         1.0         .23         28700.      8.31700E70.0            1193.       11120.      12
2.05        0.0         2000.       0.0         0.0         0.0         0.0         0.0         13
146.8       -19.273     17.142      6.0637      27.974      -.2563E-57.6883         136.74      14
.010275     .00055065.12545E-71.0               .76012                                          15
2335.041 2107.117 1879.194 1651.270 1423.346 1195.422 967.498  901.111     T1
834.723  768.336  701.949  635.561  569.174  545.318  521.461  497.605     T2
473.749  449.893  426.036  414.588  403.140  391.692  380.244  368.796     T3
357.348  327.357  316.053  312.375  311.332  311.072  311.014  311.002     T4
311.000  311.000  311.000  311.000  311.000  311.000  311.000             T5
.27056E-4.53994E-4.12582E-3.36214E-3.14076E-2.85414E-2.81182E-10.17320   R1
0.35939  0.63581  0.86734  0.96824  0.99375  .99740   0.99900  0.99965    R2
0.99989  0.99997  0.99999  1.0      1.0      1.0      1.0      1.0        R3
1.0      1.0      1.0      1.0      1.0      1.0      1.0      1.0        R4
1.0      1.0      1.0      1.0      1.0      1.0      1.0                 R5
.16777E-1.16808E-1.16822E-1.16789E-1.16782E-1.16743E-1.15970E-1.14029E-1 G1
.10367E-1.55355E-2.18775E-2.42524E-3.87951E-4.35717E-4.13314E-4.46227E-5 G2
.14338E-50.0        0.0         0.0         0.0         0.0         0.0         0.0         G3
0.0         0.0         0.0         0.0         0.0         0.0         0.0         0.0         G4
0.0         0.0         0.0         0.0         0.0         0.0         0.0                     G5
0.0         2.0         2.001       100.0                                                       A1
2700.0      2700.0      1593.0      1593.0                                                      B1
1.04        1.04        0.0         0.0                                                         C1
226.2       226.2       0.0         0.0                                                         D1
0.0         0.0         0.0         0.0                                                         E1
1.905       1.905       1.905       1.905                                                       F1
```

Figure 8.– Input data for sample case.

```
    A1            A2            A3            A4            B1            B2            B3            B4            B5
    B6            B7            B8            B9            B10           B11           B12           B13           B14
    B15           B16           C1            C2            C3            C4            C5            C6            C7
    C8            E1            E2            E3            E4            E5            E6            E7            E8
    E9            E10           E11           E12           E13           E14           E15           E16         SIGMA
    RO          OMCO           OKBAR          CHI1          VCINFI        GAMAI          TWI         DELTW         ALLOW
    HST           DCI           DDT1          DDT2          DDT3          DY1          RHO21          OMO           E17
    E18           DELTJ         E19           E20           E21           E22           E23           CJS
   RHOP          RHOCH         RHOCHA          CS            ACT         HSREF           CX            CY            A5
     A6            CK1           CK2           PS            PT2         CMBW          CMO           CMG         PHIBAR
    COW            CE            RG          TREF          HCHREF        HGREF         CKDB          CMCH          TOFF
 0.10000E 01 -0.          0.50000E 00 -0.          -0.          -0.          0.70200E 08  0.11065E 05 -0.
 0.10000E 01  0.10000E 01  0.31100E 03  0.10000E 01  0.10000E 01  0.10000E 01  0.10000E 01 -0.          0.10000E 01
 0.75000E 00 -0.          0.           0.           0.           0.           0.          -0.          -0.          0.
-0.           0.10000E 01  0.14800E 01  0.84000E-04 -0.          -0.          -0.          -0.          0.10000E 01  0.22293E 02
-0.           0.12670E-00  0.33000E 02  0.13310E 02 -0.          -0.          -0.          -0.          -0.          0.13690E-11
-0.          -0.          -0.          -0.           0.           0.          0.31100E 03 -0.          -0.          0.20000E 01
-0.          -0.           0.23000E-01  0.20000E-01  0.20000E-01  0.50000E-02 -0.          0.18802E-01  0.
 0.          -0.           0.91592E 05  0.26962E 04  0.10000E 01 -0.          0.45470E-03  0.10000E 01
 0.54450E 00  0.32050E-00  0.22500E 01 -0.          0.17014E-01 -0.83300E 02  0.13333E 01  0.10000E 01  0.17300E 01
 0.10130E 07  0.28000E 06  0.60000E 00  0.10000E 01 -0.          0.15000E 02  0.10300E 01  0.15000E 02  0.10000E 01
 0.23000E-00  0.28700E 05  0.83170E 08  0.          0.11930E 04  0.11120E 05  0.20500E 01 -0.          0.20000E 04
  KF    KG    N1    N2    NF   K2    K3    K4    LN    M2    M3    MF    J1   J2   KC5  KCT   KM1   KM2   KM3  KCM1 KCM2 KCM3 KCMF
KN1   KN2   KCN1  KCN2  KCNF  LL1   NOP   NAR  JJAR  NAROP  JJR2  JJCH
  -0     2    41    51   101    6     1     1     4    27    29    39     1    1   -0   21    2     3     4     1    1     1     1
  42    56    10    10    10    1    51     4     1     1     1    10
```

```
    NN            TTAR                HSTAR                PT2AR              QOCWAR              QRAR                RAR

     1             0.                2700.00000            1.04000           226.20000            0.                1.90500
     2             2.00000           2700.00000            1.04000           226.20000            0.                1.90500
     3             2.00100           1593.00000            0.                  0.                 0.                1.90500
     4           100.00000           1593.00000            0.                  0.                 0.                1.90500
   QQII          QQ2I          QQI           TTI           DELI          DCI          RHO          M1
0.16314E 03  0.          0.16314E 03  0.10000E 01  0.56415E-02  0.46605E 01  0.38014E-02      25
```

Figure 9.– Print-out of input data and initial calculated quantities for sample case.

N	TT	R	SNGMA	RHO	VC	RERML	PSI	QQFM
QQC	QD	QQCW	QQG	DIRML	QR	DTDYW	OMC	TDEL
CKTU	QSUB	FSUB	F1	F2	TWC	TWCAL	XIP	CHI
DTT	FSUBRAT	FSUBDIF	PHI	VCINF	ABROW	TMLO	SQQQ	PT2
CHI+YDEG/CH	YDEG/PL	YDEG/CH	PSIBAR	COIN	RIN	B	STOR	VCON
CHI+YDEG/PL	RESID	ERR	DTDYP	PSQO	FW	DTDYR	DSTOR	VARG
-VSSUB	DRES	-VSCOMB	-VSERO	QCS	QCG	QCSIN	QCGIN	QSUBIN
1	1.0000000	0.19050E 01	0.	0.38014E-02	0.47545E 01	0.16548E-01	0.76012E 00	0.
0.16314E 03	0.16314E 03	0.22620E 03	0.	0.15375E-01	0.	-0.67415E 05	0.	0.30024E-01
0.	-0.33821E-04	0.12545E-07	0.10275E-01	0.55065E-03	0.23350E 04	0.	0.33777E-01	0.17014E-01
0.20000E-01	0.47915E-06	0.12219E-07	0.10000E 01	0.30488E 01	0.27603E-01	0.18802E-01	0.	0.10400E 01
0.48037E-01	0.51618E-01	0.31023E-01	0.76012E 00	0.14680E 03	-0.19273E 02	0.34196E-00	0.76883E 01	0.17142E 02
0.68632E-01	0.13674E 03	0.	0.	0.12400E 03	-0.30524E 02	0.	0.	0.29745E 02
0.39142E-07	0.55373E 02	0.32059E-01	0.17181E-02	0.12258E 02	0.34752E 02	0.60637E 01	0.27974E 02	-0.25630E-05

M	Y	TE	RJ	RHOS	CMRGVG	XZ
1	0.	2335.041	0.27056E-04	0.32051E-00	0.16777E-01	0.
2	0.005	2107.117	0.53994E-04	0.32051E-00	0.16808E-01	0.
3	0.010	1879.194	0.12582E-03	0.32053E-00	0.16822E-01	0.
4	0.015	1651.270	0.36214E-03	0.32058E-00	0.16789E-01	0.
5	0.020	1423.346	0.14076E-02	0.32082E-00	0.16782E-01	0.
6	0.025	1195.422	0.85414E-02	0.32241E-00	0.16743E-01	0.
7	0.030	967.498	0.81182E-01	0.33868E-00	0.15970E-01	0.89637E-01
8	0.035	901.111	0.17320E-00	0.35939E-00	0.14029E-01	0.
9	0.040	834.723	0.35939E-00	0.40100E-00	0.10367E-01	0.
10	0.045	768.336	0.63581E 00	0.46292E-00	0.55355E-02	0.
11	0.050	701.949	0.86734E 00	0.51478E 00	0.18775E-02	0.
12	0.055	635.561	0.96824E 00	0.53739E 00	0.42524E-03	0.
13	0.060	569.174	0.99375E 00	0.54310E 00	0.87951E-04	0.42557E-01
14	0.065	545.318	0.99740E 00	0.54392E 00	0.35717E-04	0.
15	0.070	521.461	0.99900E 00	0.54428E 00	0.13314E-04	0.
16	0.075	497.605	0.99965E 00	0.54442E 00	0.46227E-05	0.
17	0.080	473.749	0.99989E 00	0.54448E 00	0.14338E-05	0.
18	0.085	449.893	0.99997E 00	0.54449E 00	0.	0.
19	0.090	426.036	0.99999E 00	0.54450E 00	0.	0.51523E-01
20	0.095	414.588	0.10000E 01	0.54450E 00	0.	0.
21	0.100	403.140	0.10000E 01	0.54450E 00	0.	0.
22	0.105	391.692	0.10000E 01	0.54450E 00	0.	0.
23	0.110	380.244	0.10000E 01	0.54450E 00	0.	0.
24	0.115	368.796	0.10000E 01	0.54450E 00	0.	0.
25	0.120	357.348	0.10000E 01	0.54450E 00	0.	0.52402E-01
26	0.150	327.357	0.10000E 01	0.54450E 00	0.	0.52804E-01
27	0.180	316.053	0.10000E 01	0.54450E 00	0.	0.52957E-01
28	0.210	312.375	0.10000E 01	0.54450E 00	0.	0.53007E-01
29	0.240	311.332	0.10000E 01	0.54450E 00	0.	0.53021E-01
30	0.270	311.072	0.10000E 01	0.54450E 00	0.	0.53021E-01
31	0.300	311.014	0.10000E 01	0.54450E 00	0.	0.53021E-01
32	0.330	311.002	0.10000E 01	0.54450E 00	0.	0.53021E-01
33	0.360	311.000	0.10000E 01	0.54450E 00	0.	0.53021E-01
34	0.390	311.000	0.10000E 01	0.54450E 00	0.	0.53021E-01
35	0.420	311.000	0.10000E 01	0.54450E 00	0.	0.53021E-01
36	0.450	311.000	0.10000E 01	0.54450E 00	0.	0.53021E-01
37	0.480	311.000	0.10000E 01	0.54450E 00	0.	0.53021E-01
38	0.510	311.000	0.10000E 01	0.54450E 00	0.	0.53021E-01
39	0.540	311.000	0.10000E 01	0.54450E 00	0.	0.

Figure 10.– Print-out of first time line (typical) for sample case.

REFERENCES

1. Matting, Fred W.; and Chapman, Dean R.: Analysis of Surface Ablation of Noncharring Materials with Description of Associated Computing Program. NASA TN D-3758, 1966.

2. Kennard, Earle H.: Kinetic Theory of Gases, With an Introduction to Statistical Mechanics. First ed., McGraw-Hill, New York, 1938.

3. Hidalgo, Henry: Ablation of Glassy Material Around Blunt Bodies of Revolution. ARS J., vol. 30, no. 9, Sept. 1960, pp. 806-814.

4. Baron, Judson R.: The Binary-Mixture Boundary Layer Associated with Mass Transfer Cooling at High Speeds. Tech. Rep. 160, M.I.T. Naval Supersonic Lab., Ph.D. Thesis, May 14, 1956.

5. Detra, R. W.; Kemp, N. H.; and Riddell, F. R.: Addendum to 'Heat Transfer to Satellite Vehicles Re-entering the Atmosphere.' Jet Propulsion, vol. 27, no. 12, Dec. 1957, pp. 1256-1257.

6. Hayes, Wallace D.; and Probstein, Ronald F.: Hypersonic Flow Theory. Academic Press, New York, 1959.

7. Adams, Mac C.: Recent Advances in Ablation. ARS J., vol. 29, no. 9, Sept. 1959, pp. 625-632.

8. James, Carlton S.: Experimental Study of Radiative Transport from Hot Gases Simulating in Composition the Atmospheres of Mars and Venus. AIAA J., vol. 2, no. 3, March 1964, pp. 470-475.

9. Chapman, Dean R.: An Approximate Analytical Method for Studying Entry into Planetary Atmospheres. NASA TR R-11, 1959.

10. Anon.: Evaluation of the Thermophysical Properties of the Apollo Heat Shield, Vol. I, Final Report. AVSSD-0375-67-RR, NASA CR-65754, AVCO Missiles, Space and Electronics Group, Space Systems Division, Lowell Industrial Park, Lowell, Mass., August 8, 1967.

11. Carslaw, Horatio S.; and Jaeger, J. C.: Conduction of Heat in Solids. Oxford-Clarendon Press, 1947.

12. Matting, Fred W.: General Solution of the Laminar Compressible Boundary Layer in the Stagnation Region of Blunt Bodies in Axisymmetric Flow. NASA TN D-2234, 1964.

13. Lundell, John H.; Wakefield, Roy M.; and Jones, Jerold W.: Experimental Investigation of a Charring Ablative Material Exposed to Combined Convective and Radiative Heating. AIAA J., vol. 3, no. 11, Nov. 1965, pp. 2087-2095.

14. Emmons, Howard W.; and Leigh, D.: Tabulation of the Blasius Function with Blowing and Suction. Interim Tech. Rep. 9, Combustion Aerodynamics Lab., Division of Applied Science, Harvard Univ., Nov. 1953.

NASA-Langley, 1970 —— 33 A-3614

"The aeronautical and space activities of the United States shall be conducted so as to contribute . . . to the expansion of human knowledge of phenomena in the atmosphere and space. The Administration shall provide for the widest practicable and appropriate dissemination of information concerning its activities and the results thereof."

—NATIONAL AERONAUTICS AND SPACE ACT OF 1958

NASA SCIENTIFIC AND TECHNICAL PUBLICATIONS

TECHNICAL REPORTS: Scientific and technical information considered important, complete, and a lasting contribution to existing knowledge.

TECHNICAL NOTES: Information less broad in scope but nevertheless of importance as a contribution to existing knowledge.

TECHNICAL MEMORANDUMS: Information receiving limited distribution because of preliminary data, security classification, or other reasons.

CONTRACTOR REPORTS: Scientific and technical information generated under a NASA contract or grant and considered an important contribution to existing knowledge.

TECHNICAL TRANSLATIONS: Information published in a foreign language considered to merit NASA distribution in English.

SPECIAL PUBLICATIONS: Information derived from or of value to NASA activities. Publications include conference proceedings, monographs, data compilations, handbooks, sourcebooks, and special bibliographies.

TECHNOLOGY UTILIZATION PUBLICATIONS: Information on technology used by NASA that may be of particular interest in commercial and other non-aerospace applications. Publications include Tech Briefs, Technology Utilization Reports and Notes, and Technology Surveys.

Details on the availability of these publications may be obtained from:

SCIENTIFIC AND TECHNICAL INFORMATION DIVISION

NATIONAL AERONAUTICS AND SPACE ADMINISTRATION

Washington, D.C. 20546